nature communications

Article

https://doi.org/10.1038/s41467-025-60199-1

An m^{6}A methyltransferase confers host resistance by degrading viral proteins through ubiquitination

Received: 19 September 2024

Accepted: 19 May 2025

Published online: 24 May 2025

Check for updates

Jun Guo[1,3], Tianye Zhang[1,3], Haoxin Xie[1], Haichao Hu[1], Chaonan Shi[2], Yingjie Zhao[1], Jingliang Yin[1], Gecheng Xu[1], Zechi Wu[1], Pengkun Wang[1], Jiaqian Liu[1], Peng Liu[1], Kaili Zhong[1], Feng Chen[2], Jianping Chen[1] ✉ & Jian Yang[1] ✉

Posttranscriptional and posttranslational modifications play crucial roles in plant immunity. However, how plants fine-tune such modifications to activate antiviral immunity remains unknown. Here, we report that the m^{6}A methyltransferase TaHAKAI is utilized by wheat yellow mosaic virus (WYMV) to increase viral genomic m^{6}A modification and promote viral replication. However, TaHAKAI also functions as an E3 ligase that targets the viral RNA silencing suppressor P2 for degradation and inhibits viral infection. A major allele of *TaHAKAI* in a susceptible cultivar exhibited reduced E3 ligase activity but not m^{6}A methyltransferase activity, promoting viral infection. Interestingly, TaHAKAI^R attenuates the stability of *TaWPS1* (*Wheat paired spikelets 1, WPS1*) mRNA, the negative regulator of spike development, which might increase panicle length and spikelet number by modulating its m^{6}A modification. Our study reveals a mechanism for balancing disease resistance and yield by fine-tuning m^{6}A modification and ubiquitination.

Posttranscriptional and posttranslational modifications are two important modifications that occur in organisms, both of which are associated with innate immunity[1–4], with N^6-methyladenosine (m^{6}A) and ubiquitination being among the most representative modifications. As the most prevalent internal posttranscriptional modification, m^{6}A is widely present in rRNAs, mRNAs, tRNAs, miRNAs and long noncoding RNAs and is involved in multiple functions, such as microRNA maturation, RNA stability and RNA translation[5–8]. In general, m^{6}A modification is a reversible process catalysed by a series of specific enzymes, namely, writers, readers and erasers, which together constitute the dynamic pattern of m^{6}A modification in mRNAs[9,10]. After mRNAs are translated into proteins, ubiquitin molecules in eukaryotes modify the lysine residues of proteins via ubiquitination, which can be involved in various cellular processes, including transcriptional regulation, DNA damage repair, cell metabolism and apoptosis[11,12]. The process of ubiquitination is catalysed by three different types of enzymes in sequence: ubiquitin-activating enzymes (E1), ubiquitin-conjugating enzymes (E2) and ubiquitin ligases (E3)[12,13]. In this process, E3 ligases can specifically recognise different substrates and directly or indirectly transfer ubiquitin molecules to substrate proteins, resulting in a high degree of selectivity for protein degradation[14].

Previous studies have confirmed that both m^{6}A and ubiquitination are involved in plant–virus interactions. For example, the m^{6}A eraser AtALKBH9B modulates viral genomic RNA m^{6}A abundance and promotes systemic viral infection via interaction with the coat protein of alfalfa mosaic virus (AMV)[15]. TaMTB was demonstrated to be a negative regulator of resistance to wheat yellow mosaic virus (WYMV) infection in wheat[16]. The other writer proteins NbMTA and NbHAKAI and the reader protein NbECT2A/2B/2C both suppress PepMV infection in *Nicotiana benthamiana*[17]. In eukaryotic cells, the ubiquitin–proteasome system (UPS) is the major pathway for intracellular protein degradation and functional modification, and it regulates many

[1]State Key Laboratory for Managing Biotic and Chemical Threats to the Quality and Safety of Agro-products, Key Laboratory of Biotechnology in Plant Protection of MARA, Key Laboratory of Green Plant Protection of Zhejiang Province, Institute of Plant Virology, Ningbo University, Ningbo, China. [2]State Key Laboratory of High-Efficiency Production of Wheat-Maize Double Cropping /Agronomy College, Henan Agricultural University, Zhengzhou, China. [3]These authors contributed equally: Jun Guo, Tianye Zhang. ✉e-mail: jpchen2001@126.com; nather2008@163.com

fundamental cellular processes[18,19]. Several studies have shown that the UPS constitutes a host defence mechanism to eliminate viral components. The RING-type E3 ubiquitin ligase OsRFPH2-10 interacts with the rice dwarf virus (RDV) P2 protein and mediates its degradation[20]. The E3 ubiquitin ligases NtRFP1 and SAMDC3 interact with the βC1 (Tomato yellow leaf curl China virus) and γb (Barely stripe mosaic virus) proteins, respectively, and promote degradation via the proteasome to prevent viral infection[21,22]. However, the P3 protein, encoded by rice grassy stunt virus (RGSV), induces the expression of the host effector E3 ligase P3IP1 and targets OsNRPD1a for degradation, promoting viral infection[23]. These results all point to important roles for m^{6}A and ubiquitination in the plant–virus arms race, but the relationship between m^{6}A and ubiquitination remains unknown.

HAKAI was initially identified as a RING finger E3 ubiquitin ligase that regulates E-cadherin stability[24], and its role in cell proliferation, cell growth, cell invasion and tumour progression has subsequently been extensively studied[25,26]. Recently, a *hakai* mutation was found to reduce relative m^{6}A levels in *Arabidopsis thaliana*[27], which subsequently confirmed that HAKAI interacts with the m^{6}A core members MTA, VIR, and FIP37[28], demonstrating that HAKAI is a conserved component of the methyltransferase system in plants. Biologists have also revealed that depletion of *HAKAI* reduces m^{6}A levels and alters m^{6}A-dependent functions such as sex determination in *Drosophila*[29,30], and HAKAI deficiency disrupts several subunits of the methyltransferase complex (MACOM), such as the stability of VIR, leading to impaired m^{6}A deposition[30]. Moreover, *NbHAKAI* enhances viral m^{6}A modifications and inhibits viral infection[17]. These experiments illustrate that *HAKAI* may perform both m^{6}A and ubiquitination functions in both animals and plants. However, after the invasion of pathogens, especially viruses, the precise mechanism that balances the fine regulation between HAKAI-mediated m^{6}A modification and ubiquitination remains unknown.

In China, soil-borne viral diseases of wheat caused by WYMV parasitizing *Polymyxa graminis* have caused significant yield losses in wheat production[31]. WYMV is a species of ssRNA (+) virus in the family Potyviridae that consists of two RNA strands, named RNA1 and RNA2, respectively. The optimum temperature for WYMV multiplication and systemic infection of wheat is 8 °C[32,33]. Both WYMV RNA1 and RNA2 encode a large polyprotein protein, the former being proteolytically hydrolysed to produce eight mature proteins (P3, 7 K, CI, 14 K, VPg, NIa-Pro, NIb and CP), whereas the latter is split into two proteins (P1 and P2)[32]. Previous studies have shown that the WYMV P2 protein can form aggregates in the endoplasmic reticulum membrane and recruit the viral proteins P1, P3, NIa-Pro, and VPg to the aggregates. Interestingly, P2 also interacts with P1 to recruit NIb (the replication protein of potyviruses[34]) into P2-induced aggregates[35]. Moreover, the P2 protein acts as a viral suppressor of RNA silencing and can disrupt a signal cascade of RNA silencing by interfering with the interaction between calmodulin (CAM) and calmodulin-binding transcription activator 3 (CAMTA3) to inhibit the expression of downstream RNAi silencing-related genes, such as Dicer1 (DCL1), bifunctional nuclease 2 (BN2), Argonaute protein (AGO), and RNA-dependent RNA polymerase 6 (RDR6)[36–38]. Nevertheless, a considerable amount of information about the process of P2 interactions with plants remains unknown.

In this study, we found that the m^{6}A methyltransferase TaHAKAI functions as an E3 ubiquitin ligase, and SNP analysis confirmed the existence of two haplotypes, *TaHAKAI*^{R} and *TaHAKAI*^{S}. Both TaHAKAI^R and TaHAKAI^S can perform the m^{6}A methyltransferase function, which both enhance m^{6}A modification of the WYMV viral genome and promote viral replication. Further studies revealed that both TaHAKAI^R and TaHAKAI^S can recognise and degrade the WYMV-silenced suppressor P2 protein. However, during WYMV infection, the Serine (Ser) 40 in TaHAKAI^R can be phosphorylated, which does not affect the activity of m^{6}A methyltransferase but enhances E3 ubiquitin ligase activity, leading to rapid degradation of the P2 protein and increasing wheat resistance. Finally, we found that TaHAKAI^R reduces the mRNA stability of *TaWPS1* (a negative regulator of spike development) by modulating *TaWPS1* m^{6}A modification, thereby might increasing spike length and spikelet number. In summary, our study highlights the crosstalk between m^{6}A modification and ubiquitination, which may provide an insight for the arms race between plant–virus interactions.

Results

TaHAKAI is a candidate resistance gene

We used *AtHAKAI* (At5g01160) from *Arabidopsis thaliana* as a reference sequence and identified wheat HAKAI homologues (TraesCS1A02G164400, TraesCS1D02G161400, TraesCS1B02G181200) using the Ensemble Plants website (http://plants.ensembl.org/index.html). The *TaHAKAIs* were designated *TaHAKAI-A*, *TaHAKAI-B* and *TaHAKAI-D* on the basis of chromosomal differences. To explore the role of *TaHAKAIs* in WYMV infection, we analysed the expression of *TaHAKAIs* during WYMV infection. Interestingly, *TaHAKAI-A* was significantly downregulated, whereas *TaHAKAI-B* and *TaHAKAI-D* levels were not significantly changed, suggesting that *TaHAKAI-A* is involved in the WYMV infection process (Supplementary Fig. 1A). Therefore, a single-chromosome stop-gain mutant was obtained by mutating nucleotide C to G (TCA-TGA) at CDS 403 of *TaHAKAI-A*, resulting in premature termination of translation, in the background of the wheat cultivar JING411 (Supplementary Fig. 1B). *Tahakai* and JING411 (J411) were subsequently planted in a field nursery for phenotypic observations (Yangzhou, Jiangsu, China). Compared with J411, *tahakai* presented more pronounced mosaic symptoms (Fig. 1A). Surprisingly, qRT-PCR and western blot (WB) experiments revealed lower viral RNA replication levels and greater WYMV coat protein (CP) accumulation in *tahakai* than in J411 (Fig. 1B, C and Supplementary Fig. 1C). Moreover, to gain more information about the relationship between *TaHAKAI* and WYMV, barely stripe mosaic virus (BSMV)-mediated gene silencing was employed to knock down *TaHAKAI* in the wheat 'Yangmai 158' (YM158). Wheat seedlings were inoculated with BSMV:*TaHAKAI*, BSMV:00, or BSMV:PDS (phytoene desaturase gene, which acted as a positive control). At 7 dpi, the silencing efficiency was analysed. qRT–PCR revealed that the *TaHAKAI* mRNA level was significantly lower (less than 50%) in BSMV:*TaHAKAI*-infected plants than in BSMV:00-infected plants (Supplementary Fig. 1D), indicating that *TaHAKAI* had been successfully silenced. WYMV was subsequently inoculated into wheat in which *TaHAKAI* was successfully silenced (BSMV:00 as a control), resulting in BSMV:00 + WYMV and BSMV:*TaHAKAI* + WYMV. At 7 dpi, we found that the plants infected with BSMV:*TaHAKAI* + WYMV presented more pronounced mosaic symptoms than did the control plants infected with BSMV:00 + WYMV (Fig. 1D). Moreover, qRT–PCR and WB revealed lower viral RNA replication levels and greater WYMV CP accumulation in the BSMV:*TaHAKAI* + WYMV group than in the control BSMV:00 + WYMV group (Fig. 1E, F and Supplementary Fig. 1E), suggesting that silencing *TaHAKAI* favours WYMV infection. Finally, we expressed *TaHAKAI-A* and generated transgenic *TaHAKAI* plants harbouring YM158. Two positive T_0 independent homozygous lines, *TaHAKAI*-L1-T_0 and *TaHAKAI*-L7-T_0, with high *TaHAKAI* expression levels (~12–40-fold greater than that of the control), were identified via qRT–PCR (Supplementary Fig. 1F). T_2 transgenic *TaHAKAI*-L1-T_2 and *TaHAKAI*-L7-T_2 plants were subsequently planted in a field nursery for phenotypic observation, with YM158 used as a control (Yangzhou, Jiangsu, China). We found that mosaic disease symptoms were less pronounced in *TaHAKAI*-L1-T_2 and *TaHAKAI*-L7-T_2 than in the control in the field nursery (Fig. 1G). Similarly, higher viral RNA replication levels and lower CP accumulation were also observed via qRT–PCR and WB experiments (Fig. 1H, I and Supplementary Fig. 1G). These results suggested that *TaHAKAI* positively regulates resistance to WYMV in wheat.

To further study the role of *TaHAKAI* in WYMV resistance, we sequenced *TaHAKAI* in 241 wheat varieties and analysed its

https://doi.org/10.1038/s41467-025-60199-1

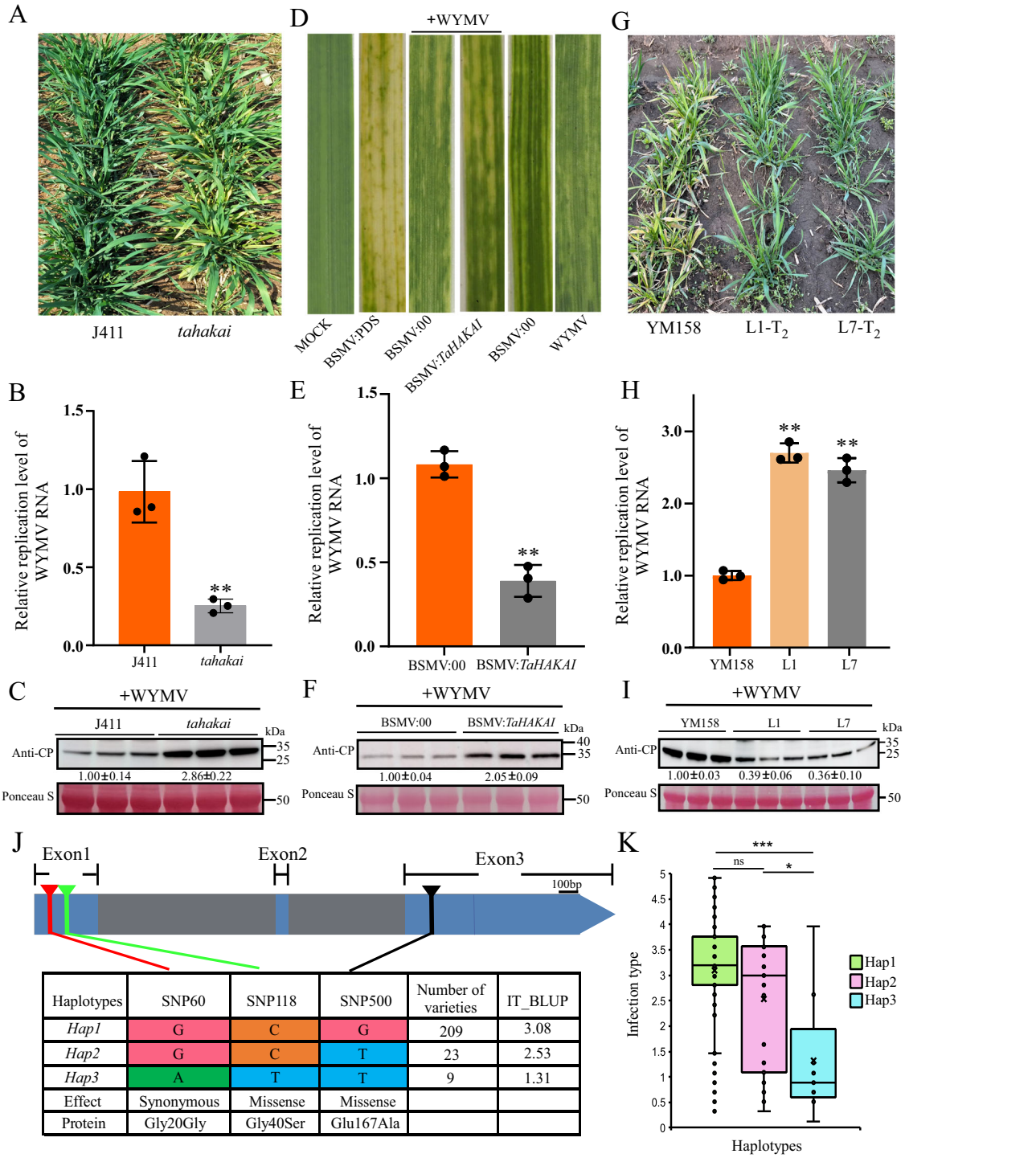

Haplotypes	SNP60	SNP118	SNP500	Number of varieties	IT_BLUP
Hap1	G	C	G	209	3.08
Hap2	G	C	T	23	2.53
Hap3	A	T	T	9	1.31
Effect	Synonymous	Missense	Missense		
Protein	Gly20Gly	Gly40Ser	Glu167Ala		

Fig. 1 | TaHAKAI is a candidate gene for resistance to wheat yellow mosaic disease. A, **G** Assessment of tahakai, L1-T2 and L7-T2 in the WYMV disease nursery at Yangzhou, Jiangsu Province; JING 411 and YM158 were used as controls. Determination of viral RNA replication levels via qRT–PCR. The value is the mean ± SD (two-sided *t*-test; three independent biological replicates were included, '**' $p < 0.01$, $p =$ '0.0033' in (**B**), '0.0008' in (**E**) and <0.0001 in **H**, respectively). **C**, **F**, **I** Determination of WYMV protein accumulation using western blot analysis. The value is the mean ± SD (three independent biological replicates were included). Ponceau staining in (**E**, **H**, **K**) shows the protein loaded in the assays. **D** Phenotypes in the fourth leaves of the plants inoculated with BSMV: 00, BSMV: PDS, BSMV: *TaHAKAI* and WYMV. **J** DNA polymorphisms in the TaHAKAI locus among 241 cultivated accessions. The TaHAKAI gene and SNPs are shown on the physical chromosome map. The blue boxes represent exons, the grey boxes represent introns, and the different coloured lines represent different SNP variant types. The different haplotypes of Haps were compared with those of Hap1. **K** Box plot of WYMV resistance comparisons between varieties harbouring the Hap1-3 haplotypes. Here, n represents the number of wheat accessions with the corresponding haplotype. Statistics: A two-sided *t*-test was performed, '*' $p < 0.05$, '***' $p < 0.001$. Hap1 vs Hap2, $p =$ '0.1363'; Hap1 vs Hap3, $p <$ '0.0001'; Hap2 vs Hap3, $p =$ '0.0053'. $n = 209$ (Hap1), 23(Hap2) and 9 (Hap3), respectively. boxplots indicate median (box centre line), 25th, 75th percentiles (box), and 5th and 95th percentiles (whiskers).

polymorphisms. We identified three SNPs in the coding region of *TaHAKAI*, performed haplotype analysis on the basis of the variation in the three SNPs, and identified a total of three haplotypes (Fig. 1J). We subsequently assessed the differences in WYMV resistance between varieties with different haplotypes, and the results revealed that varieties with Hap3 (infection type = 1.31) presented greater WYMV resistance than varieties with Hap1 (infection type = 3.08) or Hap2 (infection type = 2.58) (Fig. 1K). Hap1 and Hap2 have a G-T variant at SNP500 that leads to missense mutations. We found that Hap3 has the missense variant SNP118 (C-T), which results in mutation of glycine (Gly) to Ser, was the pivotal mutation site determining the dominant haplotype of this gene (Fig. 1J). We further studied and analysed the influence of this mutation site on *TaHAKAI* function.

TaHAKAI^R confers host resistance in a ubiquitination-dependent manner

Given that *TaHAKAI* was able to negatively regulate WYMV infection, the function of *TaHAKAI* was subsequently analysed. We found that our *TaHAKAI* clone (cloned from YM158) belongs to the Hap3 haplotype. Therefore, we subsequently designated the cloned *TaHAKAI* haplotype *TaHAKAI^R*. To reaffirm the function of TaHAKAI^R proteins, bioinformatic phylogenetic analyses of TaHAKAI proteins (TaHAKAI-A, TaHAKAI-B and TaHAKAI-D) and HAKAI proteins homologous to those of monocot and dicot species, including *Hordeum vulgare*, *Zea mays*, *Oryza sativa*, and *Arabidopsis thaliana*, were subsequently conducted. The results showed that the HAKAIs are fairly conserved in these species, as they all contain a RING and ZnF_C2H2 domain (Fig. 2A). We next performed a comparative analysis of the RING domain in these species, and the results indicated that HAKAI proteins from different species were highly conserved (identify = 96.73%) and that all HAKAIs contained a C3-H4-C4-type RING-finger domain with conserved cysteine (Cys) and histidine (His) residues (Fig. 2B), suggesting that all HAKAIs may possess E3 ubiquitin ligase activity. In order to investigate E3 ubiquitin ligase activity of TaHAKAI^R, full-length TaHAKAI^R was expressed in *Escherichia coli* as a fusion protein with maltose binding protein (MBP) and affinity-purified TaHAKAI-MBP from the soluble fraction for the in vitro ubiquitination assay (Supplementary Fig. 2A). A significant polyubiquitination signal was detected with the use of an anti-Ub antibody in the presence of TaHAKAI^R, Ub, E1 and E2 (Fig. 2C, **Lane 5**), and no polyubiquitination signal was detected in any combination lacking E1, E2 or Ub (Fig. 2C, **Lanes 1-4**). The RING motif is necessary for the E3 ligase activity of RING-type E3 ligase proteins, and an intact RING domain can affect E3 ligase activity. We also generated a single amino acid substitution allele by mutating His-111 to Tyr (H111Y) to disrupt the RING domain (TaHAKAI$^{R(H111Y)}$). This mutant completely lacked E3 ligase activity in an in vitro ubiquitination assay (Fig. 2C, **Lane 6**), further demonstrating that TaHAKAI^R is a functional E3 ligase and that the intact RING domain is required for its E3 ligase activity.

To investigate whether the resistance caused by TaHAKAI^R was dependent on its ubiquitination activity, we subsequently overexpressed TaHAKAI^R-GFP or TaHAKAI$^{R(H111Y)}$-GFP and inoculated it with WYMV in wheat protoplasts; 35S-GFP was used as a control. A time course assay was performed to determine the degree of viral replication at 6, 12, 24, 36, and 48 h. After 6 h, there was no significant difference in the level of viral replication between TaHAKAI^R-GFP, TaHAKAI$^{R(H111Y)}$ and control. However, after 12 h, the viral RNA replication level significantly increased after TaHAKAI^R-GFP and TaHAKAI$^{R(H111Y)}$-GFP overexpression compared with that of the control and reached the highest level after 24 h, followed by a subsequent decline at 36 and 48 h, although expression levels were still significantly greater than those of the control group (Fig. 2D). However, CP protein accumulation was significantly reduced after TaHAKAI^R-GFP overexpression and significantly increased after TaHAKAI$^{R(H111Y)}$-GFP overexpression compared with the control (Fig. 2E, F). Given that HAKAI was able to enhance host plant and viral genome m^{6}A modifications in plants[17,27], we assessed whether TaHAKAI^R could perform the same function. We overexpressed TaHAKAI^R-GFP and TaHAKAI$^{R(H111Y)}$-GFP in wheat protoplasts, extracted total protoplast RNA and confirmed via a dot blot assay that both TaHAKAI^R and TaHAKAI$^{R(H111Y)}$ increased the total m^{6}A levels in wheat (Fig. 2G, H). These findings suggest that TaHAKAI^R and TaHAKAI$^{R(H111Y)}$ play a role in m^{6}A modification in wheat. Moreover, we also overexpressed TaHAKAI^R-GFP or TaHAKAI$^{R(H111Y)}$-GFP and inoculated *N. benthamiana* with WYMV, extracted the viral particles and purified the viral RNA from the viral particles. Interestingly, using m^{6}A dot blotting, we found that both TaHAKAI^R and TaHAKAI$^{R(H111Y)}$ increased viral genome RNA m^{6}A modification levels equivalently compared with those in the control; however, there was no significant difference between TaHAKAI^R and TaHAKAI$^{R(H111Y)}$ (Fig. 2I, J). In conclusion, these results demonstrated that the resistance conferred to the host by TaHAKAI^R is dependent on its ubiquitination activity.

TaHAKAI^R mediates P2 degradation through the 26S proteasome system

TaHAKAI^R is a functional RING type E3 ubiquitin ligase that can negatively regulate WYMV infection. To gain insights into the function of *TaHAKAI^R* in wheat and to determine the possible mechanisms for its antiviral properties, we found that TaHAKAI^R interacted with the P2 protein in vivo via firefly luciferase complementation imaging (LCI) assays (Fig. 3A). To validate whether TaHAKAI^R also interacts with P2 in vitro, a His pulldown assay and microscale thermophoresis (MST) assay were performed using the purified TaHAKAI^R-His and P2-GST proteins. Following His pulldown, immunoblotting with an antibody revealed that TaHAKAI^R-His binds to P2-GST but not to the pGEX-GST control (Fig. 3B). Moreover, the MST assay confirmed that a dissociation constant (kd) of 16.8 nM was measured for the binding form of TaHAKAI^R + P2, whereas the kd was undetectable in the control group (Fig. 3C). In addition, we were also interested in the spatial location of TaHAKAI^R interactions with P2, and a biomolecular fluorescence complementation (BIFC) assay in H2B-RFP transgenic *N. benthamiana* revealed that TaHAKAI^R-cYFP and P2-nYFP interact in both the cytoplasm and cytoplasmic aggregates (Fig. 3D). Together, these results suggest that TaHAKAI^R interacts with P2 both in vivo and in vitro.

Generally, E3 ubiquitin ligases can direct the ubiquitination of specific target proteins as a signal for their degradation by the 26S proteasome, and ubiquitinated protein degradation is usually performed using an ATP-dependent mechanism. Our previous evidence demonstrated that the E3 ubiquitin ligase TaHAKAI^R interacts with P2 both in vivo and in vitro, providing preliminary evidence that P2 might serve as a substrate for TaHAKAI^R. Thus, we hypothesised that the P2 protein is capable of being ubiquitinated in vivo. On the basis of this assumption, we conducted a semi-in vivo protein degradation assay to quantify the effects on P2 stability. P2-GFP was expressed in wheat protoplasts. After 2 dpi, total protein was extracted, treated with the protein translation inhibitor cycloheximide (CHX), incubated and agitated in an Eppendorf thermomixer at room temperature to analyse the expression levels of the P2 protein in the presence or absence of ATP. We collected samples over 45 min and analysed protein levels by immunoblotting with an anti-GFP antibody. The results showed that the degradation speed of the P2 protein was faster in the presence of ATP than in the absence of ATP (Fig. 3E, F), suggesting that P2 protein degradation occurred partially in an ATP-dependent manner. Furthermore, in the presence of ATP, P2 protein accumulation was greater after treatment with the 26S proteasome inhibitor MG132 than after treatment with DMSO (mock-treated control) at each time point (Fig. 3G, H), indicating that the P2 protein is partially degraded by the 26S proteasome. We next investigated whether the degradation of P2 was related to TaHAKAI^R. P2-Flag was cotransfected with TaHAKAI^R-GFP in *N. benthamiana*, 35S-GFP and TaHAKAI^R(H111Y) mutant were used as a control. After 3 dpi, lower P2-Flag protein abundance was

https://doi.org/10.1038/s41467-025-60199-1

found in TaHAKAI^{R}-GFP + P2-Flag group (Fig. 3I). Furthermore, the 26S proteasome inhibitor MG132 blocked the degradation of P2 (Fig. 3I). Taken together, these results suggest that TaHAKAI^{R} interacts with P2 in vitro and in vivo and promotes the degradation of P2 via a 26S proteasome-dependent pathway.

Ubiquitination of P2 Lys554 inhibits WYMV infection

In order to identify the potential ubiquitination sites within P2, P2-GFP was transient expression in wheat protoplasts. We performed LC–MS/MS analysis and identified one residue, lysine 554 (K554), as a putative ubiquitination site (Supplementary Fig. 3A). Previous

Fig. 2 | Resistance conferred by TaHAKAI^R is dependent on ubiquitination activity. A Phylogenetic analysis of TaHAKAIs from different species. HAKAI protein sequences from *Hordeum vulgare* (Hv), *Zea mays* (Zm), *Oryza sativa* (Os), and *Arabidopsis thaliana* (At) were identified. **B** Conserved RING domain analysis of TaHAKAI-A, TaHAKAI-B and TaHAKAI-D among different plant species. The asterisk indicates the conserved RING domain amino acid residue. **C** In vitro ubiquitination assay of TaHAKAI^R. $n = 3$ biologically independent experiments. The TaHAKAI^R-mbp protein purified from *E. coli* was incubated with E1, E2, Ub, and ATP in the reactions. Immunoblot analysis was performed with anti-MBP and anti-ubiquitin antibodies. The asterisks represent the positions of the MBP and TaHAKAI^R-MBP size. **D** Determination of viral RNA replication levels via qRT–PCR at different times. The value is the mean ± SD (ANOVA with two-sided *t*-test; $n = 3$ biologically independent experiments, '**' $p < 0.01$, 'ns' not significant). The *p* value are as follows. '0.0606', '0.0551' and '0.9968' in 6 h; '0.0014', '0.0022' and '0.8653' in 12 h; '0.0043', '0.0019' and '0.6328' in 24 h; '0.0003', '0.0007' and '0.5142' in 36 h; '<0.0001', '<0.0001' and '0.8435' in 48 h. **E** Detection of WYMV protein accumulation using WB. The value is the mean ± SD ($n = 3$ biologically independent experiments). Ponceau staining was used to assess protein loading. **F** The relative abundance of the CP protein in (**E**). The value is the mean ± SD (ANOVA with two-sided *t*-tests; $n = 3$ biologically independent experiments, '*' $p < 0.05$, '**' $p < 0.01$). 35S-GFP vs TaHAKAI^R-GFP, p = '0.0070'; 35S-GFP vs TaHAKAI$^{R(H111Y)}$-GFP, p = '0.0384'; TaHAKAI^R-GFP vs TaHAKAI$^{R(H111Y)}$-GFP, p = '0.0006'. **G**, **I** Dot blotting was used to determine the m^{6}A modification levels of host RNA and viral RNA using an anti-m^{6}A antibody. MB staining of total RNA and viral RNA served as equal loading controls. **H**, **J** Quantitative statistics were performed on the m^{6}A level in (**G**, **I**). The value is the mean ± SD (ANOVA with two-sided *t*-test; $n = 3$ biologically independent experiments, '**' $p < 0.01$, 'ns' not significant). The *p* value in **H** is as follows. '<0.0001', '<0.0001'and '0.9954' in 500 ng; '0.0002', '0.0003' and 0.8885 in 250 ng. The *p* value in **J** is as follows. '0.0015', '0.0019' and '0.9695' in 500 ng; '0.0013', '0.0011' and '0.9819' in 250 ng.

studies reported that the ubiquitination of viral proteins regulates viral replication, whereas mutation of lysine (K) to arginine (R) on viral proteins does not result in ubiquitination. Thus, we first changed lysine (K) to arginine (R) within P2 and investigated whether this mutation affects P2 protein stability. After transient expression the wild-type P2-GFP and P2^{K554R}-GFP in wheat protoplasts, we collected total protein at 2 dpi and treated it with CHX and ATP at room temperature. By immunoblotting with an anti-GFP antibody, we found that the P2^{K554R} mutant protein was degraded at a slower rate than the wild-type P2 control at all time points (Fig. 4A, B). Moreover, LCI experiments demonstrated that TaHAKAI^R interacted with the P2^{K554R} mutant, excluding the possibility that the low degradability of P2^{K554R} was caused by P2^{K554R} interfering with the interaction with TaHAKAI^R (Supplementary Fig. 3B). These results suggest that the substitution of lysine 554 with arginine does not affect the ability of P2 to interact with TaHAKAI^R but decreases the P2 ubiquitination level, thereby improving P2 stability.

We next investigated the effect of *TaHAKAI^R* on the accumulation of the P2^{K554R} mutant. A semi-in vivo cell-free degradation assay was performed. Total protein from WT (YM158) and *TaHAKAI^R* OE seedlings was extracted and incubated with purified P2-MBP and P2^{K554R}-MBP proteins, respectively. The mixtures from different incubation periods were subsequently removed, and protein accumulation was measured with an anti-MBP antibody. Compared with P2-MBP, P2^{K554R}-MBP degraded more slowly when incubated with *TaHAKAI^R* OE or WT plant extracts (Fig. 4C, D). We also found that P2-MBP and P2^{K554R}-MBP incubated with protein extracts from *TaHAKAI^R* OE plants degraded more quickly than those incubated with extracts from WT plants (Fig. 4C, D). Together, the results revealed that TaHAKAI^R is responsible for P2 protein degradation.

To explore the biological effects of the P2^{K554R} mutation on WYMV infection, we altered the WYMV RNA2 sequence in pCB301-SP6-R2. This mutant pCB301-SP6-R2M vector contains a CGT sequence, with missense substitutions, at the nucleotide position 1659-1662 in WYMV RNA2 (Supplementary Fig. 3C). Then, pCB301-SP6-R2 or pCB301-SP6-R2M in vitro RNA transcripts were mixed with an equal amount pCB301-SP6-R1 RNA transcripts to inoculate wheat seedlings (pCB301-SP6-R1 + pCB301-SP6-R2 were wild-type WYMV, while pCB301-SP6-R1 + pCB301-SP6-R2M were WYMV-Mut). The results revealed that mosaic symptoms were much more severe in WYMV-Mut than in wild-type WYMV (Fig. 4E), and CP protein accumulation was also significantly greater in WYMV-Mut according to WB experiments (Fig. 4F and Supplementary Fig. 3D). These findings demonstrated that WYMV-P2^{K554R} has greater pathogenicity and is caused by the K554R mutation in the P2 protein. Taken together, these results confirmed that Lys554 of P2 was ubiquitinated and involved in TaHAKAI^R-mediated positive regulation of wheat resistance to WYMV infection.

Phosphorylated SNP enhances TaHAKAI^R E3 ubiquitination activity without affecting its ability to mediate m^{6}A methylation

As described above, the natural variation in *TaHAKAI* at SNP 118 (Gly to Ser) resulted in significant differences in resistance to WYMV (Fig. 1J, K), and we also demonstrated that TaHAKAI^R exerts its resistance by degrading the P2 protein through interactions with P2 (Fig. 3). We therefore hypothesised that this phenomenon occurs as a result of a change in the strength of TaHAKAI interactions with P2. We designated TaHAKAI in wheat 'Chinese Spring' cultivars (Hap1 haplotypes) as TaHAKAI^S and constructed a phosphomimic TaHAKAI mutant named TaHAKAI^D, as the Ser in this SNP is a potential phosphorylation site. Subsequently, TaHAKAI^S and TaHAKAI^D were C-terminally fused to LUC to generate TaHAKAI^S-Cluc and TaHAKAI^D-Cluc, respectively. Equal brightness of fluorescence intensity was observed after coexpressing TaHAKAI^R-Cluc, TaHAKAI^S-Cluc and TaHAKAI^D-Cluc with P2-Nluc in *N. benthamiana* leaves, demonstrating that TaHAKAI^R, TaHAKAI^S, and TaHAKAI^D had no effect on the strength of the interaction with the P2 protein in vivo in the LCI assay (Fig. 5A, B). Moreover, we expressed TaHAKAI^R, TaHAKAI^S, and TaHAKAI^D in *E. coli* with an MBP tag and purified them for in vitro interaction assays. MST assays were performed to investigate the binding affinity between P2 and TaHAKAI^R, TaHAKAI^S and TaHAKAI^D. The binding affinity curves of the treatment groups fitted together, which further confirmed that TaHAKAI^R, TaHAKAI^S, and TaHAKAI^D had no effect on the strength of the interaction with P2 in vitro (Fig. 5C).

Given that TaHAKAI^R, TaHAKAI^S, and TaHAKAI^D have no effect on the interaction with the P2 protein in vivo or in vitro, we investigated whether they affect the ability to degrade the P2 protein. We coexpressed P2-Flag with TaHAKAI^R-GFP, TaHAKAI^S-GFP, or TaHAKAI^D-GFP in *N. benthamiana* leaves, and 35S-GFP was used as a control. Interestingly, we observed differences in the level of P2 protein accumulation between the treatment groups. TaHAKAI^S had the weakest degradation effect on the P2 protein, whereas TaHAKAI^D had the strongest degradation effect (Fig. 5D). Because TaHAKAI^R, TaHAKAI^S, and TaHAKAI^D differ in their ability to degrade the P2 protein and TaHAKAI^R was identified as a functional E3 ubiquitin ligase (Fig. 2C), we hypothesised that there were differences in E3 ligase activity among TaHAKAI^R, TaHAKAI^S and TaHAKAI^D. To test this hypothesis, we conducted an in vitro ubiquitination assay, and the results revealed that TaHAKAI^D presented the strongest enzyme activity, followed by TaHAKAI^R, whereas TaHAKAI^S presented the weakest activity (Fig. 5E). Meanwhile, to fully substantiate this conclusion, we also conducted a phosphorylation assay to compare the differences between the TaHAKAI^S and TaHAKAI^R. Total proteins were extracted from wheat protoplast expressing TaHAKAI^S-GFP and TaHAKAI^R-GFP and enriched using GFP-Trap beads. The phosphorylation levels of the proteins were detected through WB using anti-GFP and anti-pSer antibody. The results showed that the phosphorylation levels of TaHAKAI^S were

https://doi.org/10.1038/s41467-025-60199-1

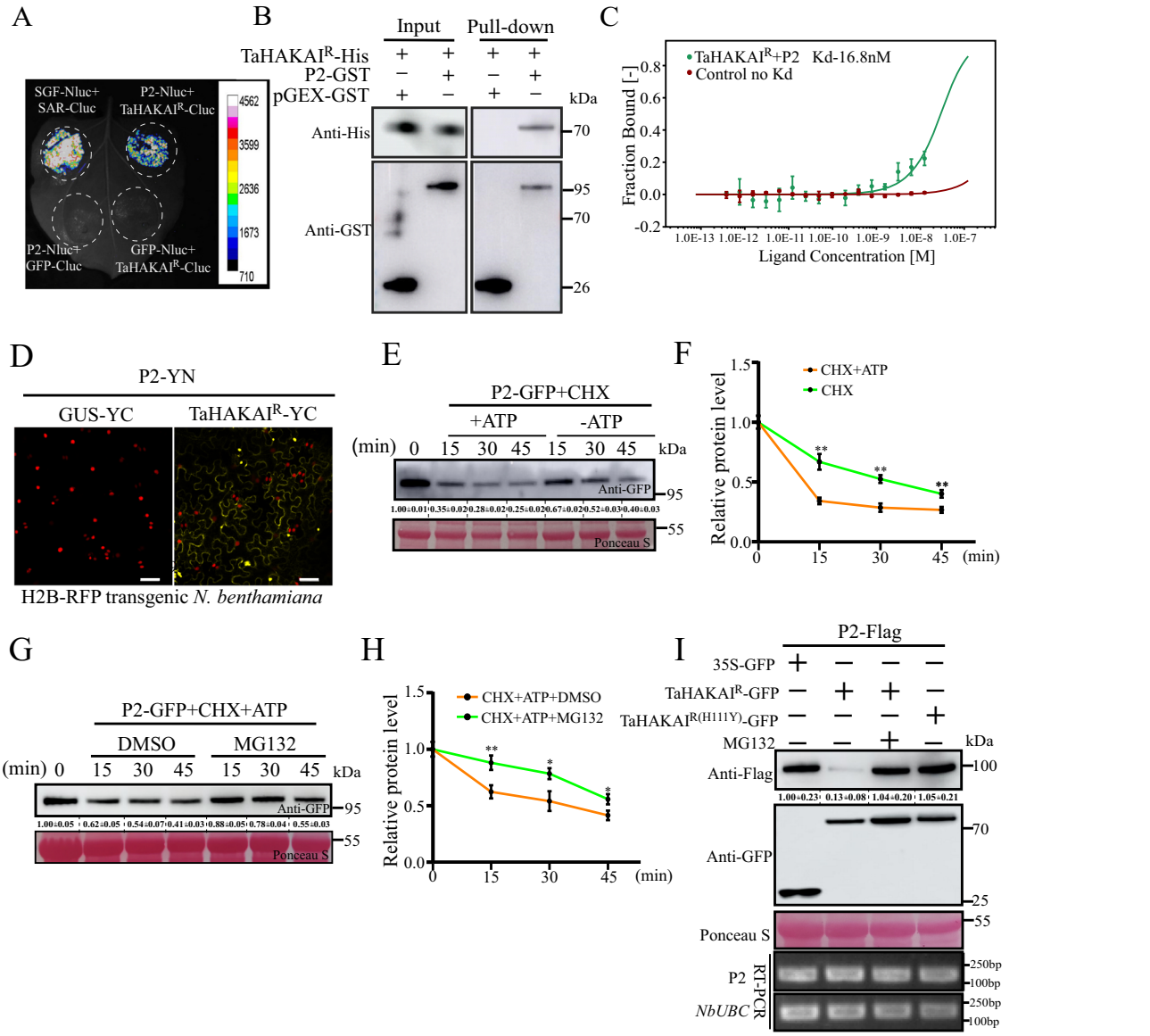

Fig. 3 | TaHAKAI^R interacts with P2 and mediates its degradation via the UPS. Verification of the interaction between TaHAKAI^R and P2 through LCI assay (**A**), pulldown assay (**B**), microscale thermophoresis assay, the values are the means ± SDs, $n = 3$ biologically independent experiments (**C**) and BiFc (Bimolecular Fluorescence Complementation), bar = 100 μm (**D**). **E** A semi-in vivo assay was used to determine the stability of the P2 protein. Total protein was extracted from wheat protoplasts at 48 h, and protein levels were analysed at different time points after 100 μm CHX treatment with a GFP antibody in the absence or presence of 20 mM ATP. **F**, **H** The relative abundance of P2-GFP. The values are the means ± SDs (ANOVA with two-sided *t*-test; $n = 3$ biologically independent experiments, '*' $p < 0.05$, '**' $p < 0.01$). The p value results in **F** are as follows. '<0.0001' in 15 min; '0.0005' in 30 min and '0.0028' in 45 min. The p value results in **H** are as follows. '<0.0067' in 15 min; '0.0138' in 30 min and '0.0166' in 45 min. **G** A semi-in vivo assay was used to determine the effect of MG132 on the stability of the P2 protein. Total protein was extracted from wheat protoplasts at 48 h, and the protein levels were analysed at different time points after treatment with 100 μM CHX and 20 mM ATP with a GFP antibody in the absence or presence of MG132. Equal amounts of dimethyl sulfoxide (DMSO) were used as a control. **I** TaHAKAI^R promotes P2 degradation via the 26S proteasome pathway. P2-Flag was coexpressed with TaHAKAI^R-GFP or TaHAKAIR$^{(H111Y)}$-GFP. The 26S proteasome inhibitor MG132 (50 μm) was added 12 h before sampling, and an equal volume of DMSO was used as a control. The relative transcript levels of *NbUBC* and P2 were determined via RT–PCR. Ponceau staining in (**E**, **G**, **I**) shows the protein loaded in the assays.

significantly lower than TaHAKAI^R (Supplementary Fig. 4A). Meanwhile, we also analysed the phosphorylation of the peptide containing this SNP (SNP40) by mass spectrometry analysis (LC-MS/MS), and the results showed that the SNP could not be phosphorylated in TaHAKAI^S, whereas it was phosphorylated in TaHAKAI^R (Supplementary Fig. 4B–D). The above results suggested that the phosphorylation level of TaHAKAI^S is lower than that of TaHAKAI^R and that the difference is attributable to SNP40. In addition, HAKAI has been reported to be an m^{6}A writer in *Arabidopsis thaliana* and *Solanum lycopersicum*. We then transiently expressed the TaHAKAI^R-GFP, TaHAKAI^S-GFP, and TaHAKAI^D-GFP in wheat protoplasts to explore their effects on the level of host RNA m^{6}A modification, with 35S-GFP used as a control. m^{6}A dot blotting was subsequently performed. The results revealed that TaHAKAIs increased the total m^{6}A level compared with that of the control, but there was no difference among TaHAKAI^R-GFP, TaHAKAI^S-GFP and TaHAKAI^D-GFP (Fig. 5F, G). These results suggest that phosphorylated SNP sites increase the E3 ubiquitination ligase activity of TaHAKAI.

We subsequently explored the effects of TaHAKAI^R and TaHAKAI^S on the viral suppressor RNA silencing (VSR) activity of P2 and determined the visible fluorescence intensity when TaHAKAI^S was coexpressed with P2. However, when TaHAKAI^R was coexpressed

https://doi.org/10.1038/s41467-025-60199-1

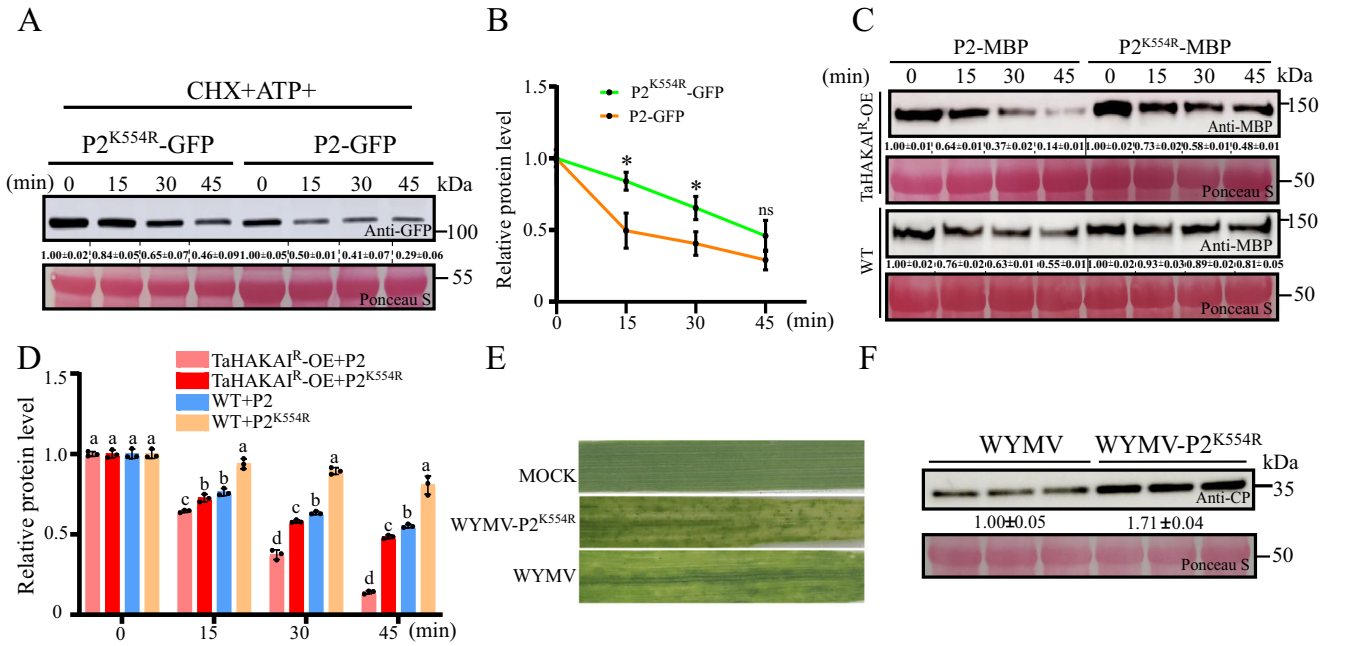

Fig. 4 | Ubiquitination of P2 at Lys554 negatively regulates WYMV infection. A A semi-in vivo assay was used to determine the stability of the P2 and P2^{K554R} proteins. Total protein was extracted from wheat protoplasts at 48 h, and the protein levels were analysed at different time points after 100 μm CHX treatment with a GFP antibody in the presence of 20 mM ATP. **B** The relative abundance of P2-GFP and P2^{K554R}-GFP. The value is the mean ± SD (ANOVA with two-sided *t*-tests; $n = 3$ biologically independent experiments included, '*' $p < 0.05$, 'ns' not significant). The *p*-value results are as follows. '0.0121' in 15 min; '0.0203' in 30 min and '0.0853' in 45 min. **C** TaHAKAI^R affects the P2 and P2^{K554R} proteins in a cell-free system. P2 and P2^{K554R} were fused to the maltose-binding protein tag (P2-MBP and P2^{K554R}-MBP). TaHAKAI^R protein was extracted from TAHAKAI^R OE plants and incubated with P2-MBP and P2^{K554R}-MBP at room temperature. An equal amount of protein extracted from WT plants (YM158) was used as a control. Protein levels were analysed at different time points by immunoblotting with an anti-MBP antibody. **D** The relative abundances of P2-MBP and P2^{K554R}-MBP. The value is the mean ± SD (ANOVA with two-sided *t*-tests; $n = 3$ biologically independent experiments included, *p* values are shown in the Source Datafile). The different letters on the bars indicate significant differences. **E** Deubiquitination at Lys-K554 promotes WYMV infection in wheat. Four leaves of wheat seedlings were inoculated with WYMV or its derivative WYMV-P2^{K554R}. Phenotypes were observed at 14 dpi. **F** Determination of WYMV protein accumulation via a WB assay. The value is the mean ± SD (three independent biological replicates were included). Ponceau staining in (**A**, **C**, **F**) shows the protein loaded in the assays.

with P2, only vaguely visible fluorescence intensity was observed (Supplementary Fig. 5A). Western blotting revealed that P2 and GFP expression levels in the TaHAKAI^S + P2 group were significantly higher and lower than those in the TaHAKAI^R + P2 group, respectively (Supplementary Fig. 5B), demonstrating that TaHAKAI^R and TaHAKAI^S had effects on the VSR activity of P2, possibly due to the difference in the ability of TaHAKAI^R and TaHAKAI^S to degrade P2. Therefore, to determine the specific biological phenomena caused by TaHAKAI^R and TaHAKAI^S, we next investigated whether TaHAKAI^R and TaHAKAI^S differ in their resistance to WYMV. The TaHAKAI^R-GFP and TaHAKAI^S-GFP were expressed and inoculated with WYMV in wheat protoplasts, and 35S-GFP was used as a control. After 48 h inoculation, compared with those in the control group, the viral RNA replication levels increased significantly after TaHAKAI^R or TaHAKAI^S expression (Fig. 5H). However, CP protein accumulation was reduced when TaHAKAI^R was overexpressed and increased when TaHAKAI^S was overexpressed compared with that in the control (Fig. 5I, J). Finally, we infiltrated *N. benthamiana* with TaHAKAI^R-GFP or TaHAKAI^S-GFP and inoculated it with WYMV. The viral particles were extracted and purified for viral genome m^{6}A detection, and 35S-GFP was used as a control. Interestingly, the results of the dot blotting assays revealed that WYMV viral RNA from TaHAKAI^R-GFP- or TaHAKAI^S-GFP-overexpressing plants presented greater m^{6}A levels than did the control; however, there was no difference between TaHAKAI^R-GFP- and TaHAKAI^S-GFP-overexpressing plants (Fig. 5K, L). These results suggest that the ubiquitination activity of phosphorylated TaHAKAI^R is increased without affecting its m^{6}A methylation ability.

TaHAKAI^R overexpression promotes field production

To determine the effects of *TaHAKAI^R*-overexpressing plants on wheat yield under field conditions, we performed trials with two T_3 lines, namely, *TaHAKAI^R*-L1-T_3 and *TaHAKAI^R*-L7-T_3, in Yangzhou city, Jiangsu Province, China, in 2024. Representative plants at the mature stage are shown in Fig. 6A, B. No differences in plant height or tiller number were noted between the *TaHAKAI^R*-OE lines and the control YM158 (Fig. 6D, E). Notably, the panicle length and number of spikelets per panicle were significantly greater in the *TaHAKAI^R*-OE lines. Specifically, the average panicle length in the *TaHAKAI^R*-OE lines was 11.32 cm and 11.59 cm, respectively, with increases of ~26% and 29%, respectively, from 8.96 cm in the control wheat cultivar YM158 (Fig. 6C, F). Moreover, the average number of spikelets per panicle in the *TaHAKAI^R*-OE lines was 19 and 20, respectively, representing increases of ~19% and 25%, respectively, from 16 in the control YM158 (Fig. 6G). We also counted the 1000-kernel weight of the *TaHAKAI^R*-OE lines. The results revealed that the mean thousand kernel weights of the *TaHAKAI^R*-OE lines were 40.91 g and 39.73 g, respectively, which were not significantly different from that of the control YM158 at 41.09 g (Fig. 6H). In addition, we investigated the agronomic traits of *tahakai* and J411, and there were no significant differences in plant height (Supplementary Fig. 6A, B, D), tiller number (Supplementary Fig. 6E) or thousand-grain weight (Supplementary Fig. 6H). However, *tahakai* presented significant disadvantages in terms of panicle length (Supplementary Fig. 6C, F) and spikelets per panicle (Supplementary Fig. 6G).

Importantly, we found that the m^{6}A level of *TaWPS1* (wheat paired spikelets 1), a negative regulator of wheat spike development[39], was

https://doi.org/10.1038/s41467-025-60199-1

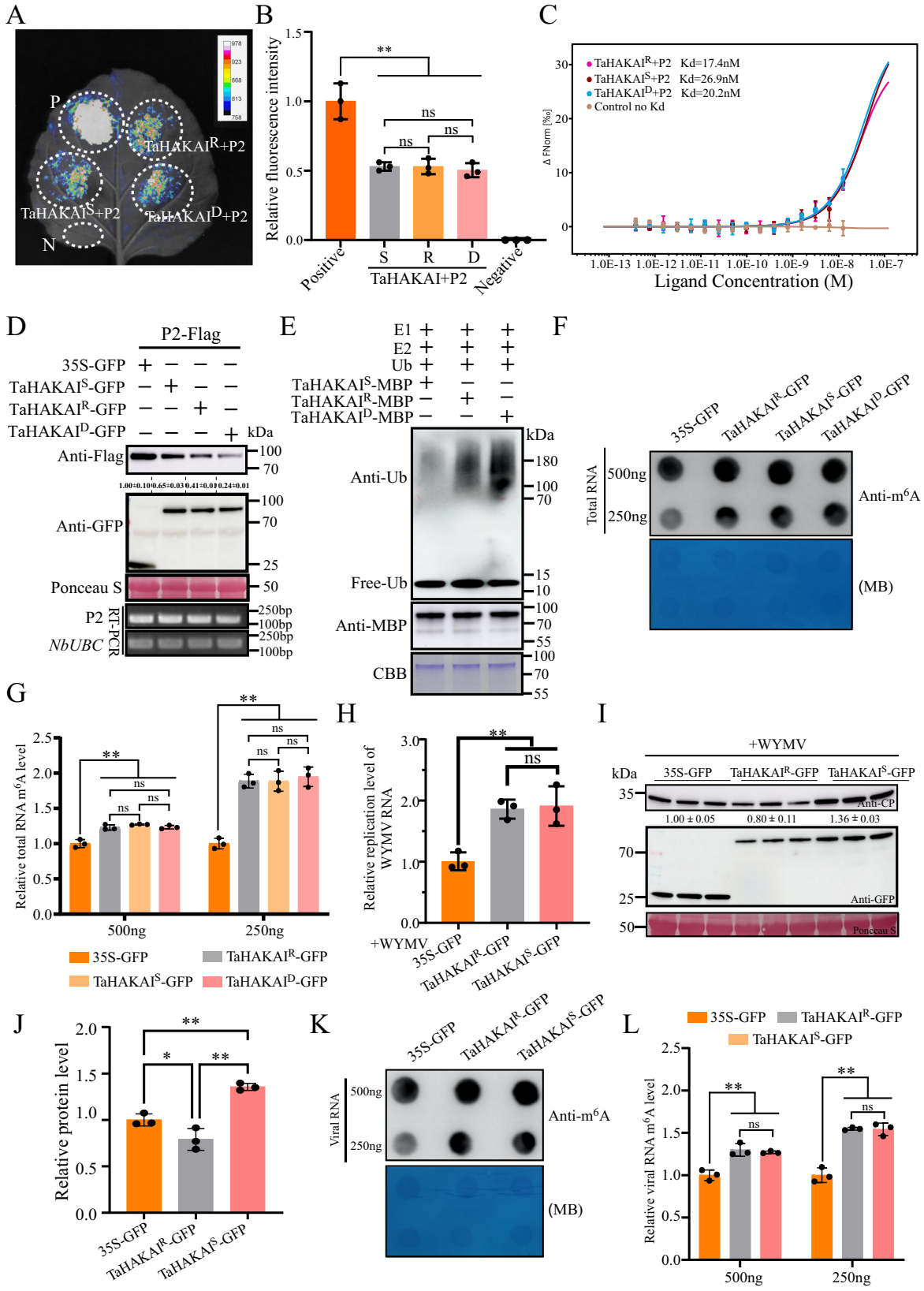

significantly increased in the *TaHAKAI*^{R}-OE lines and decreased in the *tahakai* mutant, demonstrating the ability of *TaHAKAI*^{R} to mediate the m^{6}A modification of *TaWPS1* (Fig. 6I, J). We then predicted the m^{6}A site on the cDNA sequence of *TaWPS1* using the m^{6}A prediction website (http://www.cuilab.cn/m6asiteapp) and found a high-confidence m^{6}A site on the A base at position 986 on the cDNA of *TaWPS1*. We then performed an A-G mutation at this locus to construct a *TaWPS1* mutant, TaWPS1-Mut. We analysed the mRNA stability of *TaWPS1* in *TaHAKAI*^{R} OE plants and WT plants, and the results revealed that the *TaWPS1* degradation rate was greater in *TaHAKAI*^{R} OE plants than in WT plants, indicating that *TaWPS1* was more unstable (Fig. 6K). We further analysed whether the m^{6}A site at position 986 affects its mRNA

Fig. 5 | TaHAKAI^R phosphorylation enhances its ubiquitination activity. A An LCI assay was used to confirm the interaction between TaHAKAI^R, TaHAKAI^S, and TaHAKAI^D with P2. P, positive control; N, negative control. **B** Relative fluorescence intensity of TaHAKAI^R, TaHAKAI^S, and TaHAKAI^D with P2. The *p* value is '0.7994', '0.4266', '0.9548' and '<0.0001', respectively. **C** An MST assay was used to determine the differences in the binding affinities of TaHAKAI^R-mbp, TaHAKAI^S-mbp and TaHAKAI^D-mbp for P2-GST. The MBP + P2-GST group was used as a negative control. The value is the mean ± SD, $n = 3$ biologically independent experiments. **D** Coinfiltration experiment of TaHAKAI^R, TaHAKAI^S, and TaHAKAI^D with P2. Ponceau staining was used to assess protein loading. **E** Ubiquitination assay of TaHAKAI^R, TaHAKAI^S, and TaHAKAI^D in vitro. Coomassie Brilliant Blue (CBB) assay was performed for protein loading. **F** Dot blot analysis of TaHAKAI^R, TaHAKAI^S, and TaHAKAI^D on the overall m^{6}A modification levels in wheat. **G** Quantitative statistical analysis of the m^{6}A level in (**F**). The *p* value in 500 ng: $p =$ '0.0003', $p <$ '0.0001', $p =$ '0.0002', $p =$ '0.5346', $p =$ '0.9987' $p =$ '0.6177'. The *p* value in 250 ng: $p =$ '0.0003', $p =$ '0.0002', $p =$ '0.0001', $p =$ '0.9979', $p =$ '0.7407' $p =$ '0.8307'. **H** Determination of viral RNA replication levels. 35S-GFP vs TaHAKAI^R-GFP, $p =$ '0.0053'; 35S-GFP vs TaHAKAI^S-GFP, $p =$ '0.0039'; TaHAKAI^R-GFP vs TaHAKAI^S-GFP, $p =$ '0.9471'. **I** Determination of WYMV CP protein accumulation. Ponceau staining was used to assess protein loading. **J** The relative abundance of the CP protein in (**I**). 35S-GFP vs TaHAKAI^R-GFP, $p =$ '0.0421'; 35S-GFP vs TaHAKAI^S-GFP, $p =$ '0.0039'; TaHAKAI^R-GFP vs TaHAKAI^S-GFP, $p =$ '0.0003'. **K** Dot blot analysis of TaHAKAI$^{R/S}$ on the overall m^{6}A modification levels in WYMV genomic RNA. **L** Quantitative statistics on the m^{6}A level in (**K**). The *p* value in 500 ng: $p =$ '0.0016', $p <$ '0.0027' and $p =$ '8145'. The *p* value in 250 ng: $p =$ '0.0001', $p =$ '0.0001 and $p =$ '0.9919'. In **B**, **G**, **H**, **J**, **L**, the value is the mean ± SD (ANOVA with two-sided *t*-tests; $n = 3$ biologically independent experiments, '*' $p < 0.05$, '**' $p < 0.01$, 'ns' not significant).

stability, coexpressed TaHAKAI^R with TaWPS1 and TaWPS1-mut, and subsequently tested the stability of the *TaWPS1* mRNA. The results showed that in the presence of *TaHAKAI^R*, the mRNA decay efficiency of *TaWPS1* was significantly lower in the TaWPS1-mut treatment group, suggesting that the m^{6}A modification of the A base at position 986 is detrimental to the mRNA stability of *TaWPS1* (Fig. 6L). In summary, these results indicate that *TaHAKAI^R* can improve field yield by increasing panicle length and spikelet number, possibly through m^{6}A modification of the *TaWPS1* gene.

Discussion

Soil-borne viral diseases in wheat induced by WYMV cause severe wheat yield losses[31]. Currently, the most effective measure to control this disease is to breed and plant resistant varieties, but effective resistance genes that can be used for this disease are very rare[31]. Recently, *TARD21A* and *YM2* were shown to have good resistance to WYMV, suggesting that there is great potential for mining candidate genes for resistance to WYMV[40,41]. In plants, HAKAI was identified as an m^{6}A methyltransferase involved in root growth and development[27]. HAKAI also increases viral m^{6}A modification and inhibits PepMV RNA accumulation[17]. However, the role of HAKAI in plant antiviral responses remains largely unexplored, especially for WYMV. Our results provide comprehensive evidence that *TaHAKAI^R* is a candidate gene for WYMV resistance in wheat. To confirm this possibility, we obtained a *tahakai* mutant that exhibited high susceptibility to WYMV. Similar results were obtained when BSMV-mediated gene silencing technology was used. Conversely, we assessed *TaHAKAI^R* in stable high-expression plants, which presented high resistance to WYMV (Fig. 1). These results clearly indicate that *TaHAKAI^R* plays a key role in plant defence against viruses. However, we found that *TaHAKAI^R* promoted viral replication in *tahakai* plants, BSMV-silenced wheat and *TaHAKAI^R* OE plants (Fig. 1B, E, H). Previous studies have demonstrated that hMPV and SARS-CoV-2 in human cells undergo m^{6}A modifications, which favour viral replication[42,43] and that *HAKAI* is associated with m^{6}A methyltransferases in plants[27]. We hypothesise that similar mechanisms may exist for WYMV and that these mechanisms are mediated by *TaHAKAI^R*.

In mammalian cells, HAKAI was originally identified as the E3 ubiquitin ligase that mediates the ubiquitination of the E-cadherin complex[24]. Moreover, HAKAI was also identified as a component of MACOM that not only functions to stabilise MACOM components in *Drosophila* and human cells[30] but is also involved in plant root development in *A. thaliana*[27,28]. However, the function of HAKAI as an E3 ubiquitin ligase in plants has not yet been reported. In our current investigation, we demonstrated via an in vitro ubiquitination assay that TaHAKAI^R is a functional E3 ubiquitin ligase (Fig. 2D), suggesting that TaHAKAI^R is involved in ubiquitination-related processes in wheat. This finding has been instrumental in greatly expanding research on the function of TaHAKAI in plants. Moreover, we determined that the ability of TaHAKAI^R to confer host resistance is dependent on its ubiquitination activity; however, interestingly, TaHAKAI$^{R(H111Y)}$ was able to promote viral infection at the level of both viral replication and protein accumulation (Fig. 2E, F). As previously hypothesised, we attributed this result to the ability of TaHAKAI^R to mediate m^{6}A modifications on the viral genome. We subsequently confirmed that TaHAKAI^R enhances viral genome m^{6}A modifications, thereby increasing viral replication, via an m^{6}A dot blot assay (Fig. 2E–G). Two strategies involving the UPS have been extensively reported in the study of both plant and animal viruses: (i) the UPS can recognise viral proteins and induce their degradation to inhibit viral infection[20,21,44], and (ii) the UPS can also be exploited by smart viruses that have evolved sophisticated strategies to favour their own infection[18,23,45,46]. In our study, we provide compelling evidence that TaHAKAI^R mediates viral protein P2 degradation via the UPS. Through in vivo and in vitro interaction experiments, we confirmed that TaHAKAI^R can interact with P2. Furthermore, P2 can be ubiquitinated in vivo, and this process is partially dependent on TaHAKAI^R (Fig. 3). This result is consistent with previous reports that P2 can be degraded by ubiquitination in *N. benthamiana*[47,48]. Generally, polyubiquitin chains are linked at the Lys48 residue as the primary signal for 26S proteasome-mediated degradation of the substrate[49,50]. Using LC–MS/MS, semi-in vivo and cell-free degradation assays, and biological characterisation, we demonstrated that ubiquitination occurs on the Lys554 residue of P2. Although the P2^{K554R} mutation did not completely abolish P2 ubiquitination, it indeed attenuated the effect of TaHAKAI^R on P2 accumulation and facilitated WYMV infection (Fig. 4). This finding suggests that there may be other ubiquitination sites present on the P2 protein, but at a minimum, our results demonstrate that residue Lys554 is one of the primary effector sites. Moreover, exploring whether Lys554 is highly conserved across different WYMV strains and revealing a mechanism of broad-spectrum resistance via ubiquitination to target the P2 proteins of other *Bymoviruses* is important.

Phosphorylation and ubiquitination are two of the most abundant and best-studied PTMs, and their interactions have received widespread attention. In mammalian cells, several excellent reviews have discussed the crosstalk between phosphorylation and ubiquitination[51–53]. Moreover, in plants, many fascinating studies on the crosstalk between phosphorylation and ubiquitination have been performed[54–57], suggesting a high frequency of communication and interactions. In addition, the consequences of the phosphorylation of an E3 ligase may vary as discussed above. In this study, we identified a critical natural variant of *TaHAKAI*. This SNP caused a Gly to Ser amino acid substitution at position 40 of *TaHAKAI*. Given that Ser is a potential phosphorylation site, this finding suggests that phosphorylation may modulate TaHAKAI function. However, we did not observe a change in the interaction pattern of TaHAKAI$^{R/S}$ with P2 (Fig. 5A–D), which differs from the flg22-induced FLS2-PUB12/13 interaction dependent on PUB12/13 phosphorylation by BAK1[56]. Instead, we clarified the alteration in E3 ligase activity upon phosphorylation. The strong E3 ligase activity of TaHAKAI^R resulted in faster degradation of the targeted P2 protein (Fig. 5E). Similarly, others have reported that

https://doi.org/10.1038/s41467-025-60199-1

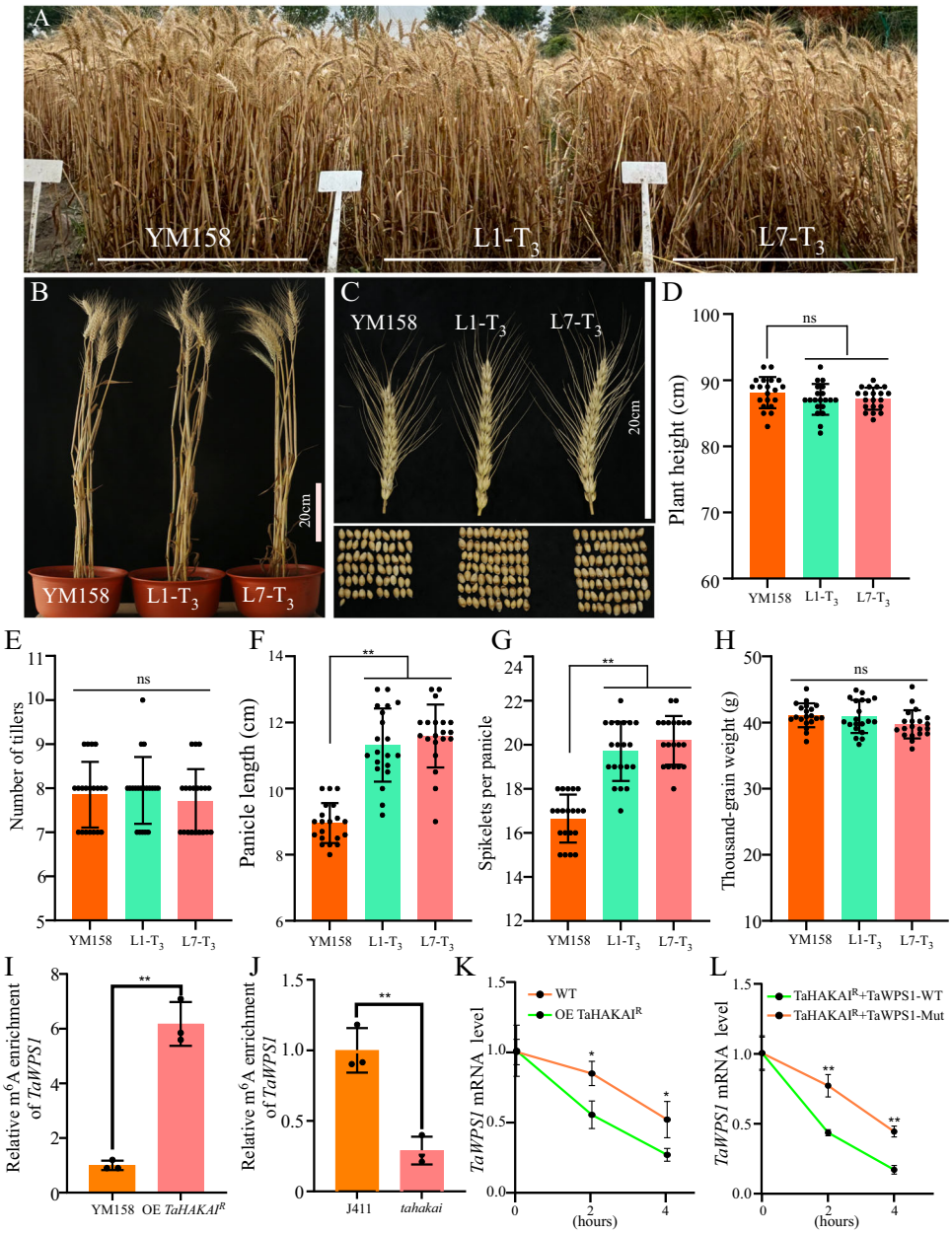

Fig. 6 | Investigation of the field agronomic traits of TaHAKAI^R-overexpressing plants. Photographs of mature WT and *TaHAKAI^R OE* plants in the field (**A**) and in pots in the field (**B**), as well as in spikelets (**C**) in Yangzhou city, Jiangsu Province. (**D**) Plant height (YM158 vs L1-T$_3$, p = '0.2343'; YM158 vs L7-T$_3$, p = '0.2998'), (**E**) number of tillers (YM158 vs L1-T$_3$, p = '0.878'; YM158 vs L7-T$_3$, p = '0.7503'), (**F**) panicle length (YM158 vs L1-T$_3$, p < '0.0001'; YM158 vs L7-T$_3$, p < '0.0001'), (**G**) spikelets per panicle (YM158 vs L1-T$_3$, p < '0.0001'; YM158 vs L7-T$_3$, p < '0.0001'), and (**H**) thousand-grain weight (YM158 vs L1-T$_3$, p = '0.9479'; YM158 vs L7-T$_3$, p = '0.0914') of WT and *TaHAKAI^R* OE plants in the field test (n = 20). Differences were evaluated via two-tailed Student's t-test, '**' p < 0.01, 'ns' no significance). Bar, 20 cm. The all values are the means ± SDs. **I**, **J** m^{6}A–IP–qPCR assay of *TaWPS1* in *TaHAKAI^R* OE or tahakai plants. Total RNA was extracted from wheat plants incubated with anti-m^{6}A or IgG (negative control) for IP. Differences were evaluated via two-tailed Student's t-test, '**' p < 0.01). The value is the mean ± SD (ANOVA with two-sided t tests; n = 3 biologically independent experiments). For **I**, YM158 vs OE *TaHAKAI^R*, p = '0.0004'. For **J**, J411 vs *tahakai*, p = '0.0027'. **K** mRNA stability assay of *TaWPS1*. Actinomycin D was injected into *TaHAKAI^R* OE and WT wheat leaves, and the stability of the *TaWPS1* mRNA was analysed by taking samples immediately after the injection, i.e., 0 h, and samples were taken at 2-h intervals a total of three times. The value is the mean ± SD (ANOVA with two-sided t tests; n = 3 biologically independent experiments). The p value results are as follows. '0.017' in 2 h; '0.034' in 4 h. **L** The wild-type (WT) or mutated (986A-G) coding region of *TaWPS1* was cloned and inserted into the expression vector and coexpressed with TaHAKAI^R in wheat protoplasts. The value is the mean ± SD (ANOVA with two-sided t tests; n = 3 biologically independent experiments). The p value results are as follows. '0.0006' in 2 h; '0.0006' in 4 h.

PUB25/26 phosphorylation by CPK28 enhances the E3 ligase activity that targets BIK1 for degradation[57]. As we demonstrated above, TaHAKAI plays a role in m^{6}A modification in wheat (Fig. 2E–G), which prompted us to elucidate the m^{6}A methylation differences mediated by TaHAKAI^R and TaHAKAI^S. In this study, we did not observe differences in host total RNA or viral RNA m^{6}A modifications or in viral replication levels (Fig. 5F, G, I). Conversely, high levels of viral accumulation were present in TaHAKAI^S, which we attributed to the presence of weak E3 ligase activity in TaHAKAI^S (Fig. 5E, H). Consequently, we confirmed that phosphorylated TaHAKAI exhibits stronger E3 ligase activity. Given that this phosphorylation is derived from the natural *TaHAKAI* variant, we believe that it has sufficient potential for

https://doi.org/10.1038/s41467-025-60199-1

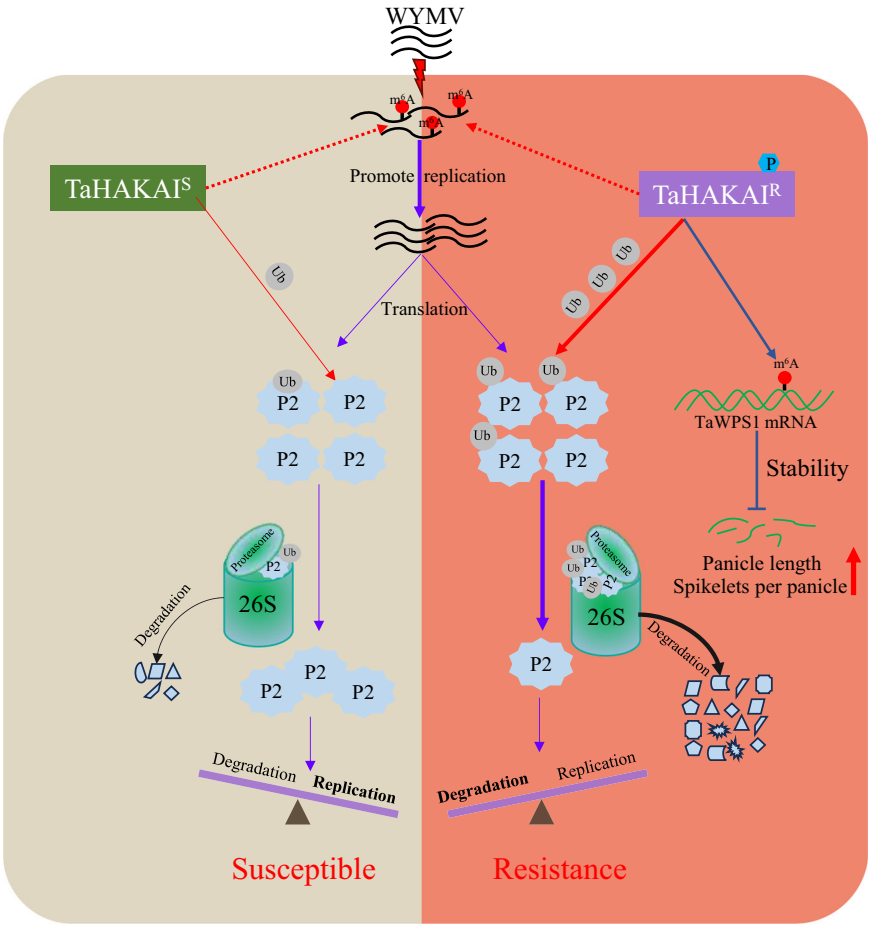

Fig. 7 | A working model illustrating the role of TaHAKAI in WYMV replication. During WYMV infection, TaHAKAI^R is phosphorylated by the host, whereas TaHAKAI^S is not phosphorylated. TaHAKAI^R and TaHAKAI^S, which are m^{6}A writers in plants, were used by WYMV to increase WYMV genomic m^{6}A modifications and promote viral replication. The viral RNA-silenced suppressor P2 protein is subsequently translated from the viral genome and subsequently recognised by the E3 ligases TaHAKAI^R and TaHAKAI^S to perform ubiquitination functions to degrade the P2 protein. TaHAKAI^S possesses weaker ubiquitination activity, leading to reduced P2 protein degradation, thus promoting viral replication. In contrast, phosphorylated TaHAKAI^R has increased ubiquitination activity, leading to the degradation of most of the P2 protein and, therefore, the inhibition of WYMV infection. Moreover, TaHAKAI^R also increases the m^{6}A modification levels of *TaWPS1* and reduces *TaWPS1* mRNA stability, thereby increasing panicle length and spikelet number. The thicknesses of the solid blue and red arrows represent the strength of the function, and the dotted arrows represent unknown specific mechanisms.

integration into wheat breeding programmes to increase WYMV resistance.

Recently, the role of the m^{6}A machinery in plant growth and development has gradually been elucidated. In *A. thaliana*, the m^{6}A methyltransferase complex has been reported to be involved in essential plant growth and development processes, such as seedling growth[27], root vascular formation[27], embryo development[58], and dominance[59]. More importantly, m^{6}A demethylation by the human RNA demethylase FTO caused ~50% increases in yield and biomass in rice and potato[60]. These findings indicate that the modulation of m^{6}A methylation is potentially an efficient strategy for crop improvement. TaHAKAI^R is a methyltransferase that can increase the panicle length and number of spikelets per panicle of wheat in the field (Fig. 6C, F, G). These findings suggest that *TaHAKAI^R* may be involved in m^{6}A modification of genes related to wheat growth and development, especially spike development. *TaWPS1* is a spike development-associated gene that leads to an increase in the number of spikelets when mutated and is a negative regulator of wheat spike development[39]. More importantly, our results revealed that TaHAKAI^R mediates the m^{6}A modification of *TaWPS1* and reduces its mRNA stability (Fig. 6I–K). Combined with the agronomic trait phenotypes of *TaHAKAI^R*, we hypothesised that *TaWPS1* may be a target gene of *TaHAKAI^R*, which enhances the m^{6}A modification of *TaWPS1* to the detriment of *TaWPS1* mRNA stabilisation, thereby increasing the number of spikelets. However, more experimental evidence is needed to support this hypothesis.

In summary, we propose a working model for the role of *TaHAKAI* in WYMV replication. Upon WYMV infection, TaHAKAI^R haplotypes are phosphorylated at Ser40, whereas TaHAKAI^S haplotypes are not phosphorylated. Both TaHAKAI^R and TaHAKAI^S were used by WYMV to perform m^{6}A functions, equivalently to enhance viral genomic m^{6}A and promote viral replication. However, during the translation process, both TaHAKAI^R and TaHAKAI^S can function as an E3 ligase to interact with the viral RNA silencing suppressor P2 and promote its degradation via the 26S proteasome. However, TaHAKAI^S has relatively weak E3 activity and can degrade only a small portion of the P2 protein, thus promoting WYMV infection. In contrast, phosphorylated TaHAKAI^R has relatively strong E3 ligase activity and degrades most of the P2 protein, thus inhibiting WYMV infection. Moreover, TaHAKAI^R also increased the m^{6}A modification of *TaWPS1* and reduced *TaWPS1* mRNA stability, thereby increasing panicle length and spikelet number (Fig. 7).

Methods

Plant material and growth conditions

N. benthamiana and wheat 'Yangmai 158' (YM158, susceptible cultivar) were grown in pots containing nutrient substrate soil in an incubation environment at 25 °C with 16 h/8 h light/dark cycles and 65% humidity. *N. benthamiana* at the six-leaf stage was used for location analysis of genes and subsequent coexpression experiments. Constitutive expression of 35S promoter in YM158 was used to construct OE-*TaHAKAI*^{R} plants. For the field experiments, the JING411, *tahakai*, YM158, and *TaHAKAI*^{R}-OE lines were planted in a field nursery in Yangzhou city, Jiangsu Province, China, from 2023 to 2024.

Plasmid construction

The full-length WYMV protein was cloned from a WYMV infectious clone. TaHAKAI^{R} and TaHAKAI^{S} were cloned from YM158 and the wheat 'Chinese Spring' cultivar, respectively. For the BIFC assay, the TaHAKAI^{R} and P2 CDSs were amplified via attB1 and attB2, and the PCR products were purified and introduced into pDONOR 207 by the BP reaction. The TaHAKAI^{R}-207 and P2-207 plasmids were subsequently cloned and inserted into pGTQL1211 (Yn) and pGTQL1221 (Yc) to generate TaHAKAI^{R}-YC and P2-YN, respectively. For the LCI assay, TaHAKAI$^{R/S/D}$ and P2 CDSs were amplified and inserted into pCambia1300-N/Cluc to generate TaHAKAI$^{R/S/D}$-Cluc and P2-Nluc, respectively. For the pulldown assay, the TaHAKAI^{R} and P2 CDSs were amplified and inserted into pET-32a and pGEX-4T-2 to obtain TaHAKAI^{R}-His and P2-GST. For the in vitro ubiquitination assay, the TaHAKAI$^{R/S/D}$ CDS was cloned and inserted into pMAL-c2x to obtain TaHAKAI$^{R/S/D}$-MBP. The recombinant plasmids used for the LCI assay, pulldown assay, in vitro ubiquitination assay, and subcellular location were constructed via in-fusion one-step cloning. Plasmid construction of *TaWPS1* and the m^{6}A site mutant of *TaWPS1*. Potential m^{6}A modification sites on *TaWPS1* were predicted using the Smart website (http://www.cuilab.cn). The overlap technique was used to mutate the A modified by m^{6}A on *TaWPS1* mRNA to G. Finally, TaWPS1 and TaWPS-Mut were constructed into the pCambia 1305 vector using homologous recombination. All primers used in this study are listed in Supplementary Data 1.

Wheat protoplast isolation and viral inoculation

The WYMV infectious cDNA clones pCB301-SP6-R1 and pCB301-SP6-R2, which contain full-length sequence information for RNA1 and RNA2, were prepared[33]. Wheat protoplasts were isolated from wheat seedlings (YM158) at the two-leaf stage as previously described[61]. Plasmid protoplast transformation and WYMV inoculation were performed according to the protocols for plant protoplast extraction and transformation kit RTU4052 (Real-Times (Beijing) Biotechnology Co., Ltd, Beijing China). In brief, 10–20 μg of plasmid DNA, either alone or in a 1:1:1 ratio, was gently mixed with 100 μL of protoplast mixture in a 1.5 mL centrifuge tube. An equal volume of preprepared transformation solution I was added to the centrifuge tube, the bottom of the tube was gently tapped to mix, and the tube was allowed to stand at room temperature (25 °C) for 5–15 min. A total of 440 μl of Solution II was then added gently and thoroughly mixed to terminate the transformation process; the mixture was then centrifuged at 100 × *g* for 1–2 min at room temperature, and as much of the supernatant as possible was removed. Then, 500 μl of Solution II was added to gently resuspend the protoplasts, which were centrifuged at 100 × *g* for 1 min at room temperature, and as much of the residual supernatant was removed as possible. Finally, 1 ml of Solution V was added to the precipitate, which was gently resuspended, after which the centrifuge tube was placed horizontally and incubated in the dark. For WYMV inoculation, incubation was conducted at a low temperature (8 °C) to create the most suitable environment, and the WYMV RNA replication level at different time points (12, 24, 36, and 48 h) and protein levels (24 h) were determined. For single-plasmid transient expression (P2-GFP and P2^{K554R}-GFP), the protoplasts were incubated at room temperature overnight.

WYMV inoculation in the laboratory

The wheat cultivar YM158 (susceptible cultivar, S) was selected as a material to examine the role of *TaHAKAI*^{R} in WYMV infection. The WYMV infectious cDNA clones pCB301-SP6-R1 and pCB301-SP6-R2, which contain full-length sequence information for RNA1 and RNA2, were generated from rub-inoculated WYMV[33]. Two-leaf-stage wheat seedlings were prepared for WYMV inoculation and maintained at 8 °C for 7 dpi.

BSMV-mediated gene silencing

To silence *TaHAKAI* expression in wheat, a specific 300-bp fragment of the *TaHAKAI* sequence containing the *NotI* and *PacI* restriction enzyme sites was obtained via RT–PCR and inserted into the BSMV-γ vector to generate γ-TaHAKAI. The plasmids BSMV-α, BSMV-β, BSMV-γ, and γ-TaHAKAI were linearised via restriction enzyme digestion (*MluI*, *SpeI*, *MluI*, and *BSSHII*) and transcribed in vitro using a Message T7 in vitro transcription kit (Ambion Austin, TX; Promega, Shenzhen) following the manufacturer's instructions. The transcription products were inoculated with BSMV (BSMV-γ, BSMV: TaHAKAI, or BSMV: PDS) into wheat at the two-leaf stage and incubated at 25 °C under 16 h/8 h alternating light/dark conditions and high humidity in a constant-temperature incubator. BSMV: PDS was used as a positive control.

RNA extraction, qRT–PCR and western blot analysis

Total RNA was extracted from the wheat samples using the FastPure® Cell/Tissue Total RNA Isolation Kit V2, RC112 (Vazyme Biotech Co., Ltd, Nanjing, China). One microgram of total RNA was used for cDNA synthesis with an *Evo M-MLV* RT Kit with gDNA Clean for qPCR AG11705 (ACCURATE BIOTECHNOLOGY (HUNAN) CO., LTD, Changsha, China). Quantitative real-time (qRT) PCR was performed with SYBR Green Premix Pro Taq HS qPCR Kit AG11701 (ACCURATE BIOTECHNOLOGY (HUNAN) CO., LTD., Changsha, China) using the ABI system (Applied Biosystems, Foster City, CA, USA). At least three biological and four technical replicates were performed per sample. The qRT-PCR data were normalised using *TaCDC (XM_020313450)* as an internal reference gene, and the results were analysed using the $2^{-\Delta\Delta CT}$ method. All primers used for RT–PCR are listed in supplementary data 1. For western blot analysis, the total protein of the extracted samples was mixed with lysis solution containing 6% SDS, boiled in water at 95 °C for 10 min and incubated on ice for 10 min. The protein samples were analysed using SDS–PAGE and transferred to nitrocellulose membranes. The blots were subsequently incubated for 60 min in blocking buffer containing 5% skim milk in 1 × PBS, and specific primary antibodies (CP, GFP, Flag, and MBP) and horseradish peroxidase (HRP)-conjugated secondary antibodies (anti-mouse and anti-rabbit) were used. The infotmation and dilution ratios of these antibodies were anti-CP (prepared by Huaan Bio, Hangzhou, Zhejiang, China, stored in our lab, 1:2000), anti-m^{6}A (Synaptic Systems, Göttingen, Germany, Cat. No. 202 003, 1:2000), anti-phosphoserine (Abcam, United Kingdom, Cat. No. Ab9332, 1:2000), anti-Ub (Abcam, United Kingdom, Cat. No. Ab134953, 1:5000), anti-GFP (TransGen Biotech, Beijing, China, Cat. No. HT801, 1:5000), anti-Flag (TransGen Biotech, Beijing, China, Cat. No. HT201, 1:5000), anti-His (TransGen Biotech, China, Cat. No. HT501, 1:5000), anti-GST (TransGen Biotech, China, Cat. No. HT601, 1:5000), anti-MBP (TransGen Biotech, China, Cat. No. HT701, 1:5000) and anti-secondary mouse (Abbkine Scientific Co., Ltd., California, USA, Cat. No. A21010, 1:5000), anti-secondary rabbit (Abbkine Scientific Co., Ltd, California, USA, Cat. No. A21020, 1:5000). The blot signal was detected and visualised using an Amersham Imager 680 machine (GE Healthcare BioSciences, Pittsburgh, PA, USA).

Firefly luciferase complementation imaging (LCI) assay

The TaHAKAI$^{R/S/D}$-Nluc and P2-Cluc plasmids were subsequently transformed into *Agrobacterium* strain GV3101. After transformation, the mixture was shaken at 28 °C for 14–16 h, centrifuged at 8000 × *g* for 5 min to collect the organisms, diluted with buffer (10 mM MES, 10 mM $MgCl_2$, 200 mM AS) and adjusted to an OD_{600} of 0.5. TaHAKAI$^{R/S/D}$ was infiltrated with an equal volume of a 1:1 mixture of P2 in *N. benthamiana* leaves and incubated at 25 °C. After 72 h, the infiltrated portion was placed in a 0.2 mM fluorescein (Thermo Scientific, USA) solution for 5 min and then viewed under chemiluminescence with an imaging system (Tanon). P2-Nluc+GFP-Cluc and GFP-Nluc+TaHAKAI$^{R/S/D}$-Cluc were used as negative controls, and SAR-Cluc+SGF-Nluc was used as a positive control.

Pull-down assay

To confirm the interaction between TaHAKAI^{R} and P2 in vitro, recombinant protein expression was induced in *E. coli* BL21 (DE3) cells by adding 1 mM isopropyl-β-D-thiogalactoside (IPTG) at 16 °C overnight. Protein purification and purity testing were performed by Huaan Bio (Hangzhou, Zhejiang, China). In total, 0.25 mg of purified TaHAKAI^{R}-His protein or P2-GST protein was incubated with 50 μl of His-tagged protein purification gel (BEENbio, Shanghai, China) at 4 °C with slow rotation for 2 h. After completion of the reaction, a portion of the supernatant was aspirated as input, and the remaining purification gel was washed with 1× PBS six times and boiled for 8 min in 2× SDS–PAGE loading buffer. Finally, the proteins were subjected to western blot assays with anti-His (TransGen Biotech, China, Cat. No. HT501, 1:5000) and anti-GST antibodies (TransGen Biotech, China, Cat. No. HT601, 1:5000).

Microscale thermophoresis assay (MST)

The interaction as well as the strength of the interaction between TaHAKAI$^{R/S/D}$ and P2 was determined using a Monolith NT.115 kit according to the manufacturer's instructions (NanoTemper Technologies, Munich, Germany). Briefly, purified P2 protein was labelled using the Monolith NT Protein Labelling Kit according to the manufacturer's instructions and mixed with a gradient dilution of purified TaHAKAI^{R}, TaHAKAI^{S} or TaHAKAI^{D} protein. The finished mixed protein samples were added into the capillaries of the kit when the reaction was finished, and the equilibrium dissociation constant (KD) value was calculated using NanoTemper analysis software.

Bimolecular fluorescence complementation (BiFC)

For BiFC, *Agrobacterium* strain GV3101 containing the plasmids TaHAKAI^{R}-YC and P2-YN was centrifuged at 8000 × *g* for 5 min to collect the organisms, which were subsequently diluted with buffer (10 mM MES, 10 mM $MgCl_2$, 200 mM AS), and the OD_{600} was adjusted to 0.5 for coexpression. An equal volume of a 1:1 mixture of TaHAKAI^{R}-YC and P2-YN was infiltrated into H2B-RFP transgenic *N. benthamiana* leaves and incubated at 25 °C. After 48 h, the spatial location of TaHAKAI^{R} with P2 was observed under a confocal laser scanning microscope. GUS-YC + P2-YN was used as a negative control.

In vitro ubiquitination assay

For the E3 ligase activity assay, total YM158 extracts were extracted with nondenaturing extraction buffer (50 mM Tris-MES, pH 8.0, 0.5 M sucrose, 1 mM $MgCl_2$, 10 mM EDTA, 5 mM DTT, and protease inhibitor cocktail) and preincubated with purified TaHAKAI$^{R/S/D}$-MBP protein for the prior assay[62,63]. MBP magnetic beads were rotated with the mixture at 4 °C for 1 h. The beads were retained and subjected to an in vitro ubiquitination reaction. The ubiquitination reaction mixture contained E1 (wheat E1), E2 (AtUBC8), 2 μg/μL ubiquitin (U-100At, Boston Biochem, USA) and purified TaHAKAI$^{R/S/D}$-MBP in 1× reaction buffer (50 mM Tris-HCl, pH 7.4; 10 mM $MgCl_2$; 5 mM ATP; 2 mM DTT). The samples were subsequently incubated at 30 °C for 2 h, and E3 ligase activity was assessed via western blotting with anti-Ub (Abcam, United Kingdom, Cat. No. Ab134953, 1:5000) and anti-MBP (TransGen Biotech, China, Cat. No. HT701-01, 1:5000) antibodies[62,64].

Semi-in vivo and in vivo degradation assays

For the semi-in vivo protein degradation assay, P2-GFP and P2^{K554R}-GFP were expressed in wheat protoplasts, and total proteins were extracted using the nondenaturing extraction buffer described previously, with the addition of ATP (Thermo Fisher, R0441) at final concentrations of 20 mM and 50 μM of the 26S proteasome inhibitors MG132 (Sangon Biotech, T510313) and DMSO (Sangon Biotech, A610163). The mixture was placed in an Eppendorf Thermomixer machine at room temperature (25 °C) for incubation, and samples were taken at 15-min intervals and incubated in boiling water with SDS sample buffer for 10 min three times for no more than 45 min. The protein degradation levels were analysed via western blotting.

To analyse the ability of TaHAKAI^{R} to mediate the degradation of the P2 protein via the 26S proteasome, TaHAKAI^{R}-GFP and TaHAKAI$^{R(H111Y)}$-GFP were coexpressed with P2-Flag (the pGTQL1221 plasmid contains a Flag tag at the C-terminus, hereafter referred to as P2-Flag) in *N. benthamiana*, and 35S-GFP was used as a negative control. A final concentration of 50 μM MG132 was added 24 h before sampling, and DMSO was used as a control. Total protein was extracted, boiled for 10 min, and analysed for P2 protein degradation via western blotting with anti-Flag (TransGen Biotech, Beijing, China, Cat. No. HT201, 1:5000) and anti-GFP (TransGen Biotech, Beijing, China, Cat. No. HT801, 1:5000) antibodies.

Identification of the ubiquitination and phosphorylation site through LC-MS/MS

The P2-GFP, TaHAKAI^{S}-GFP and TaHAKAI^{R}-GFP fusion was transiently expressed in wheat protoplasts and then enriched through immunoprecipitation with GFP-Trap beads. The enriched protein was detected through WB using anti-GFP (TransGen Biotech, Beijing, China, Cat. No. HT801, 1:5000) or anti-body anti-phosphoserine (Abcam, United Kingdom, Cat. No. Ab9332, 1:2000). Then, the protein slices in fresh CCB-stained gel were excised and plated into a 96-well microtitre plate. Excised slices were first destained twice with 200 μl of 50 mM NH4HCO3 and 50% acetonitrile and then dried twice with 200 μl of acetonitrile. The gel pieces were rehydrated in 10 mM dithiothreitol and incubated at 56 °C for 60 min. Gel pieces were again dehydrated in 100% acetonitrile and rehydrated with 55 mM iodoacetamide in the dark for 45 min. Afterwards, the dried pieces of gel were incubated in ice-cold digestion solution (trypsin 12.5 ng/μl and 20 mM NH_4HCO_3) for 20 min and then transferred into a 37 °C incubator for digestion overnight. Finally, peptides in the supernatant were collected after extraction twice with 200 μl extract solution (5% formic acid in 50% acetonitrile). The peptide solution described above was dried under the protection of N_2 and prepared for ubiquitination and phosphorylation site identification. Tandem mass spectra were extracted by Proteome Discoverer software (Thermo Fisher Scientific, version 3.0.) Tandem mass spectra were searched against Human database, assuming the digestion enzyme trypsin. Mass error was set to 10 ppm for precursor ions and 0.02 Da for fragment ions. Carbamidomethyl of cysteine was specified as fixed modification. Oxidation of methionine and acetylation of lysine were specified as variable modifications. Number of max missed cleavage sites was set to 2. The acceptance criteria for identifications were that the false discovery rate (FDR) should be less than 1% for peptides and proteins.

Extraction of WYMV particles

In brief, 100 g of leaves was ground into a powder in liquid nitrogen, and precooled 0.5 mol/L borate buffer (0.001 M EDTA, pH 9.0) was added to form a homogenate, which was filtered through double-layer gauze. The extracts were then centrifuged at 10,000 × *g* for 15 min at

4 °C, and one-fourth of the volume of carbon tetrachloride was added to the supernatant. The mixture was stirred vigorously for 5 min and then centrifuged again at 10,000 × *g* for 15 min after being allowed to rest for 30 min on ice. The supernatant was mixed with 6% PEG6000, 3% NaCl and 1% Triton-X 100; agitated at 4 °C for 2 h; and allowed to stand overnight. Centrifugation at 10,000 × g was then performed for 30 min, and the precipitate was suspended in 10 mL of 0.01 mol/L potassium borate buffer. The supernatant was subsequently collected via centrifugation at 10,000 × *g* for 30 min. Finally, the supernatant was added to an ultracentrifuge tube containing one-third the volume of 20% sucrose (2% Triton-X 100) and centrifuged at 38,000 × *g* for 2 h. Then, the precipitate was dissolved in 1 mL of sterilised water to obtain the purified viral particles.

Dot blot assay

For RNA preparation, total RNA from wheat protoplasts was extracted using the HiPure Plant RNA Kit (Magen, Guangzhou, China), whereas WYMV genomic RNA was obtained from purified WYMV viral particles. In brief, the following steps were performed: 100 µl of viral particle suspension was mixed with 500 µl of TE buffer (1 M Tris-HCl, 0.5 M EDTA, and 5 M NaCl), an equal volume of phenol was added, and the mixture was shaken for 3 min and then centrifuged at 12,000 × *g* at 4 °C for 3 min. The supernatant was added to an equal volume of chloroform and centrifuged again with shaking. Then, the supernatant was mixed with an equal volume of isopropanol and placed in a freezer at −20 °C overnight. Next, the mixture was centrifuged at 12,000 × *g* for 15 min at 4 °C and eluted with 70% ethanol three times. Finally, 35 µl of sterilised water was added to dissolve the sample to obtain the purified RNA.

For the m^{6}A dot blot assay, the wheat protoplast RNA and viral genome RNA were diluted into different concentration gradients and denatured at 90 °C for 5 min. The mixtures were quickly chilled on ice for 10 min and then spotted onto a Hybond-N + membrane, followed by UV crosslinking at 254 nm with 0.12 J/cm^2 as described above[16]. The membranes containing the RNA blots were subsequently incubated with blocking buffer (1x TBS, 0.02% Tween-20, and 5% nonfat milk) for 1 h, followed by incubation with specific m^{6}A primary antibodies (Synaptic Systems, Göttingen, Germany, Cat. No. 202 003, 1:2000) and rabbit secondary antibodies (Abbkine, A21010). The blots were then washed three times with 1x PBS for 8 min each. The RNA was stained with 0.1% methylene blue (Solarbio, G1300) and imaged with white light in a gel imaging system.

m^{6}A RNA immunoprecipitation and qPCR

The detailed methods used for m^{6}A RNA immunoprecipitation have been described previously[16]. Briefly, 75 µg of total RNA from wheat plants was prepared. For the reactions, 10 µg of m^{6}A antibody was used for treatment, and the absence of m^{6}A antibody was used as a negative control. For m^{6}A-IP-qPCR, 2.5 µg of the purified mRNA sample was fragmented with RNA fragmentation buffer (10 mM Tris-HCl, pH 7.0, and 10 mM $ZnCl_2$) and incubated at 95 °C for 3 min. The reaction was subsequently terminated by the addition of 50 mM EDTA and placed on ice. A total of 10% of the total RNA was used as input, and the remainder was used for immunoprecipitation. The input mRNAs and IP mRNAs were reverse transcribed as described above. Relative mRNA enrichment was measured via qRT-PCR and normalised to the input level.

mRNA stability assay

For the mRNA stability assay, TaWPS1-GFP, TaWPS1-mu-GFP, and TaHAKAI^R-GFP were cotransfected into wheat protoplasts and incubated overnight at room temperature. Then, 20 µg/mL actinomycin D (Sigma, A4262) was dissolved in ddH_2O and added to the wheat protoplasts. After treatment for 30 min, the wheat protoplasts were sampled and used as time 0 controls, and subsequent samples were harvested every 2 h. The mRNA levels of genes were subsequently determined via qRT-PCR. For the *TaWPS1* mRNA stability assay in WT and *TaHAKAI*^{R} OE plants. 20 µg/mL of actinomycin D was injected into wheat leaves, and the time of injection was labelled as 0 h, and subsequent samples were harvested every 2 h.

Statistical analysis

The significant differences among different treatments were statistically determined by ANOVA comparison and followed by a Student's *t*-test if ANOVA analysis was significant at $p < 0.05$ or $p < 0.01$ using GraphPad Prism 9 software or Image J.

Reporting summary

Further information on research design is available in the Nature Portfolio Reporting Summary linked to this article.

Data availability

Data supporting the findings of this work are available within the paper and its supplementary information files. The raw dataset of LC-MS/MS was submitted to the ProteomeXchange database with the accession number PXD056650 and PXD062647, respectively. Source data are provided with this paper.

References

1. Ivanov, P. & Anderson, P. Post-transcriptional regulatory networks in immunity. *Immunol. Rev.* **253**, 253–272 (2013).
2. Liu, J., Qian, C. & Cao, X. Post-translational modification control of innate immunity. *Immunity* **45**, 15–30 (2016).
3. Davis, M. E. & Gack, M. U. Ubiquitination in the antiviral immune response. *Virology* **479-480**, 52–65 (2015).
4. Prall, W. et al. Pathogen-induced m6A dynamics affect plant immunity. *Plant Cell* **35**, 4155–4172 (2023).
5. Tang, J., Chen, S. & Jia, G. Detection, regulation, and functions of RNA N(6)-methyladenosine modification in plants. *Plant Commun.* **4**, 100546 (2023).
6. Yue, H., Nie, X., Yan, Z. & Weining, S. N6-methyladenosine regulatory machinery in plants: composition, function and evolution. *Plant Biotechnol. J.* **17**, 1194–1208 (2019).
7. Cantara, W. A. et al. The RNA modification database, RNAMDB: 2011 update. *Nucleic Acids Res* **39**, D195–D201 (2011).
8. Wei, W., Ji, X., Guo, X. & Ji, S. Regulatory role of N(6) -methyladenosine (m(6) A) methylation in RNA processing and human diseases. *J. Cell Biochem.* **118**, 2534–2543 (2017).
9. Jiang, X. et al. The role of m6A modification in the biological functions and diseases. *Signal. Transduct. Target Ther.* **6**, 74 (2021).
10. Panneerdoss, S. et al. Cross-talk among writers, readers, and erasers of m(6)A regulates cancer growth and progression. *Sci. Adv.* **4**, eaar8263 (2018).
11. Mooney, E. C. & Sahingur, S. E. The ubiquitin system and A20: implications in health and disease. *J. Dent. Res.* **100**, 10–20 (2021).
12. Buetow, L. & Huang, D. T. Structural insights into the catalysis and regulation of E3 ubiquitin ligases. *Nat. Rev. Mol. Cell Biol.* **17**, 626–642 (2016).
13. Zhang, Y. & Zeng, L. Crosstalk between ubiquitination and other post-translational protein modifications in plant immunity. *Plant Commun.* **1**, 100041 (2020).
14. Stone, S. L. Role of the ubiquitin proteasome system in plant response to abiotic stress. *Int. Rev. Cell Mol. Biol.* **343**, 65–110 (2019).
15. Martínez-Pérez, M. et al. Arabidopsis m(6)A demethylase activity modulates viral infection of a plant virus and the m(6)A abundance in its genomic RNAs. *Proc. Natl. Acad. Sci. USA* **114**, 10755–10760 (2017).
16. Zhang, T. et al. N6-methyladenosine RNA modification promotes viral genomic RNA stability and infection. *Nat. Commun.* **13**, 6576 (2022).

17. He, H. et al. m(6)A modification of plant virus enables host recognition by NMD factors in plants. *Sci. China Life Sci.* **67**, 161–174 (2024).
18. Luo, H. Interplay between the virus and the ubiquitin-proteasome system: molecular mechanism of viral pathogenesis. *Curr. Opin. Virol.* **17**, 1–10 (2016).
19. Glickman, M. H. & Ciechanover, A. The ubiquitin-proteasome proteolytic pathway: destruction for the sake of construction. *Physiol. Rev.* **82**, 373–428 (2002).
20. Liu, L. et al. OsRFPH2-10, a ring-H2 finger E3 ubiquitin ligase, is involved in rice antiviral defense in the early stages of rice dwarf virus infection. *Mol. Plant* **7**, 1057–1060 (2014).
21. Shen, Q. et al. Tobacco RING E3 ligase NtRFP1 mediates ubiquitination and proteasomal degradation of a geminivirus-encoded βC1. *Mol. Plant* **9**, 911–925 (2016).
22. Li, Z. et al. SAMDC3 enhances resistance to Barley stripe mosaic virus by promoting the ubiquitination and proteasomal degradation of viral γb protein. *N. Phytol.* **234**, 618–633 (2022).
23. Zhang, C. et al. A bunyavirus-inducible ubiquitin ligase targets RNA polymerase IV for degradation during viral pathogenesis in rice. *Mol. Plant* **13**, 836–850 (2020).
24. Fujita, Y. et al. Hakai, a c-Cbl-like protein, ubiquitinates and induces endocytosis of the E-cadherin complex. *Nat. Cell Biol.* **4**, 222–231 (2002).
25. Aparicio, L. A., Valladares, M., Blanco, M., Alonso, G. & Figueroa, A. Biological influence of Hakai in cancer: a 10-year review. *Cancer Metastasis Rev.* **31**, 375–386 (2012).
26. Liu, Z., Wu, Y., Tao, Z. & Ma, L. E3 ubiquitin ligase Hakai regulates cell growth and invasion, and increases the chemosensitivity to cisplatin in non-small-cell lung cancer cells. *Int J. Mol. Med.* **42**, 1145–1151 (2018).
27. Růžička, K. et al. Identification of factors required for m(6) A mRNA methylation in Arabidopsis reveals a role for the conserved E3 ubiquitin ligase HAKAI. *N. Phytol.* **215**, 157–172 (2017).
28. Zhang, M. et al. Two zinc finger proteins with functions in m(6)A writing interact with HAKAI. *Nat. Commun.* **13**, 1127 (2022).
29. Wang, Y. et al. Role of Hakai in m(6)A modification pathway in Drosophila. *Nat. Commun.* **12**, 2159 (2021).
30. Bawankar, P. et al. Hakai is required for stabilization of core components of the m(6)A mRNA methylation machinery. *Nat. Commun.* **12**, 3778 (2021).
31. Yang, J. et al. Advances in understanding the soil-borne viruses of wheat: from the laboratory bench to strategies for disease control in the field. *Phytopathol Res.* **4**, 27 (2022).
32. Namba, S., Kashiwazaki, S., Lu, X., Tamura, M. & Tsuchizaki, T. Complete nucleotide sequence of wheat yellow mosaic bymovirus genomic RNAs. *Arch. Virol.* **143**, 631–643 (1998).
33. Zhang, F. et al. Construction and biological characterization of an infectious full-length cDNA clone of a Chinese isolate of Wheat yellow mosaic virus. *Virology* **556**, 101–109 (2021).
34. Urcuqui-Inchima, S., Haenni, A. L. & Bernardi, F. Potyvirus proteins: a wealth of functions. *Virus Res.* **74**, 157–175 (2001).
35. Sun, L., Andika, I. B., Shen, J., Yang, D. & Chen, J. The P2 of Wheat yellow mosaic virus rearranges the endoplasmic reticulum and recruits other viral proteins into replication-associated inclusion bodies. *Mol. Plant Pathol.* **15**, 466–478 (2014).
36. Wang, Y. et al. A calmodulin-binding transcription factor links calcium signaling to antiviral RNAi defense in plants. *Cell Host Microbe* **29**, 1393–1406.e1397 (2021).
37. Wang, Y., Gong, Q., Jin, Z., Liu, Y. & Hong, Y. Linking calcium and RNAi signaling in plants. *Trends Plant Sci.* **27**, 328–330 (2022).
38. Chen, D. et al. The P2 protein of wheat yellow mosaic virus acts as a viral suppressor of RNA silencing in Nicotiana benthamiana to facilitate virus infection. *Plant Cell Environ.* **47**, 4543–4556 (2024).
39. Zhang, J. et al. Genetic and transcriptomic dissection of an artificially induced paired spikelets mutant of wheat (Triticum aestivum L.). *Theor. Appl. Genet.* **135**, 2543–2554 (2022).
40. Liu, P. et al. A papain-like cysteine protease-released small signal peptide confers wheat resistance to wheat yellow mosaic virus. *Nat. Commun.* **14**, 7773 (2023).
41. Mishina, K. et al. Wheat Ym2 originated from Aegilops sharonensis and confers resistance to soil-borne Wheat yellow mosaic virus infection to the roots. *Proc. Natl. Acad. Sci. USA* **120**, e2214968120 (2023).
42. Lu, M. et al. N(6)-methyladenosine modification enables viral RNA to escape recognition by RNA sensor RIG-I. *Nat. Microbiol.* **5**, 584–598 (2020).
43. Zhang, X. et al. Methyltransferase-like 3 modulates severe acute respiratory syndrome coronavirus-2 RNA N6-methyladenosine modification and replication. *mBio* **12**, e0106721 (2021).
44. Rojas, V. K., Park I. W. Role of the ubiquitin proteasome system (UPS) in the HIV-1 Life Cycle. *Int. J. Mol. Sci.* **20**, 2984 (2019).
45. Gao, G. & Luo, H. The ubiquitin-proteasome pathway in viral infections. *Can. J. Physiol. Pharm.* **84**, 5–14 (2006).
46. Tang, Q., Wu, P., Chen, H. & Li, G. Pleiotropic roles of the ubiquitin-proteasome system during viral propagation. *Life Sci.* **207**, 350–354 (2018).
47. Chen, C. et al. TBtools: an integrative toolkit developed for interactive analyses of big biological data. *Mol. Plant* **13**, 1194–1202 (2020).
48. Chen, D. et al. The P1 protein of wheat yellow mosaic virus exerts RNA silencing suppression activity to facilitate virus infection in wheat plants. *Plant J.* **116**, 1717–1736 (2023).
49. Sadanandom, A., Bailey, M., Ewan, R., Lee, J. & Nelis, S. The ubiquitin-proteasome system: central modifier of plant signalling. *N. Phytol.* **196**, 13–28 (2012).
50. Callis, J. The ubiquitination machinery of the ubiquitin system. *Arabidopsis Book* **12**, e0174 (2014).
51. Hunter, T. The age of crosstalk: phosphorylation, ubiquitination, and beyond. *Mol. Cell* **28**, 730–738 (2007).
52. Nguyen, L. K., Kolch, W. & Kholodenko, B. N. When ubiquitination meets phosphorylation: a systems biology perspective of EGFR/MAPK signalling. *Cell Commun. Signal.* **11**, 52 (2013).
53. Filipčík, P., Curry, J. R. & Mace, P. D. When worlds collide-mechanisms at the interface between phosphorylation and ubiquitination. *J. Mol. Biol.* **429**, 1097–1113 (2017).
54. Stone, S. L., Anderson, E. M., Mullen, R. T. & Goring, D. R. ARC1 is an E3 ubiquitin ligase and promotes the ubiquitination of proteins during the rejection of self-incompatible Brassica pollen. *Plant Cell* **15**, 885–898 (2003).
55. Stone, S. L., Arnoldo, M. & Goring, D. R. A breakdown of Brassica self-incompatibility in ARC1 antisense transgenic plants. *Science* **286**, 1729–1731 (1999).
56. Lu, D. et al. Direct ubiquitination of pattern recognition receptor FLS2 attenuates plant innate immunity. *Science* **332**, 1439–1442 (2011).
57. Wang, J. et al. A regulatory module controlling homeostasis of a plant immune kinase. *Mol. Cell* **69**, 493–504.e496 (2018).
58. Zhong, S. et al. MTA is an Arabidopsis messenger RNA adenosine methylase and interacts with a homolog of a sex-specific splicing factor. *Plant Cell* **20**, 1278–1288 (2008).
59. Bodi, Z. et al. Adenosine methylation in arabidopsis mRNA is associated with the 3′ end and reduced levels cause developmental defects. *Front. Plant Sci.* **3**, 48 (2012).
60. Yu, Q. et al. RNA demethylation increases the yield and biomass of rice and potato plants in field trials. *Nat. Biotechnol.* **39**, 1581–1588 (2021).

61. Yang, J. et al. Chinese wheat mosaic virus-derived vsiRNA-20 can regulate virus infection in wheat through inhibition of vacuolar- (H(+))-PPase induced cell death. *N. Phytol.* **226**, 205–220 (2020).
62. Wang, R. et al. An ORFeome of rice E3 ubiquitin ligases for global analysis of the ubiquitination interactome. *Genome Biol.* **23**, 154 (2022).
63. Wang, J. et al. The E3 ligase OsPUB15 interacts with the receptor-like kinase PID2 and regulates plant cell death and innate immunity. *BMC Plant Biol.* **15**, 49 (2015).
64. Ning, Y. et al. The SINA E3 ligase OsDIS1 negatively regulates drought response in rice. *Plant Physiol.* **157**, 242–255 (2011).

Acknowledgements

We are grateful to Professor Yuese Ning and Xiaoman You, Institute of Plant Protection, Chinese Academy of Agricultural Sciences, for providing plasmids related to ubiquitination experiments, including E1, E2 and Ub. This work was supported by National Key Research and Development Programme of China (2023YFD1400300), China Agriculture Research System from the Ministry of Agriculture of the P.R. China (CARS-03), Zhejiang Provincial Natural Science Foundation of China (grant no. LDQ23C140001), National Natural Science Foundation of China (32372488), National Natural Science Foundation of China (32472495), Foundation of Zhejiang Province High-level Talent Project (Grant No.2022R52022) and Shandong Province First-class Discipline Construction “811"Project.

Author contributions

J.G., T.Z., H.H., J.C., F.C. and J.Y. conceived the research project and designed the experiment. J.G., H.X., C.S., Y.Z., J.Y., G.X., Z.W., and P.W. performed the experiment. J.G., J.L., K.Z., P.L. and J.Y. analysed the data. J.G., C.S., F.C. and J.Y. wrote the manuscript.

Competing interests

The authors declare no competing interests.

Additional information

Supplementary information The online version contains supplementary material available at https://doi.org/10.1038/s41467-025-60199-1.

Correspondence and requests for materials should be addressed to Jianping Chen or Jian Yang.

Peer review information *Nature Communications* thanks Brian Gregory, Zhihua Hua and the other, anonymous, reviewer(s) for their contribution to the peer review of this work. [A peer review file is available].